Cell treatment and surface functionalization using the atmospheric pressure glow discharge plasma torch (APGD-*t*)

Sara Yonson
Chemical Engineering
McGill University, Montreal

Under the supervision of:
Prof. Sylvain Coulombe
Prof. Richard Leask

Submitted April 2006

A thesis submitted to McGill University in partial fulfillment of the requirements of the degree of Master in Engineering.

Your file Votre référence
ISBN: 978-0-494-28635-7
Our file Notre référence
ISBN: 978-0-494-28635-7

Abstract

The atmospheric pressure glow discharge plasma torch (APGD-*t*) was used to treat cell cultures to investigate potential reactions with biological tissue. The plasma jet successfully detached HAAE-1 and HepG2 cells from a culture surface. The cells surrounding the void did not show any morphological damage after treatment. The detached HepG2 cells were transplanted to a new vessel, where they reattached. A viability assay showed the transplanted cells had functioning mitochondria up to 7 days after exposure to the plasma jet. These cells were also shown to have a permeabilized cell membrane for 4 hours after treatment, with resealing of the cell membrane occurring within 24 hours of transplantation. This work could be useful for localized tissue removal, and the injection of foreign DNA and RNA into cells for gene therapy.

In separate experiments, sterilized bacterial grade polystyrene (BGPS) was functionalized with the plasma jet to improve cell adhesion. The contact angle of treated BGPS decreased from 93° to 35°, likely due to the addition of polar oxygen and nitrogen groups to the surface. The width of the functionalized track was visualized using the adhesion of HAAE-1 cell cultures, and was found to correspond to approximately double the diameter of the plasma jet. Direct plasma micropatterning using the APGD-*t* could replace the masks and chemicals required in present photolithographic techniques.

Résumé

Une torche à plasma froid miniature opérant à pression atmosphérique (APGD-*t*) a été utilisée pour traiter des cellules en culture afin de créer un modèle représentatif des réactions probables entre le plasma et un tissu biologique. L'application du plasma sur des cellules HAAE-1 et HepG2 cultivées sur une surface polymérique a permis de détacher certaines de ces cellules de la surface. Les cellules sont demeurées sur la surface et n'ont subit aucun changement morphologique. Les cellules HepG2 qui se sont détachées ont été transplantées sur une nouvelle surface polymérique, où elles se sont rattachées et sont demeurées viables jusqu'à 7 jours suivant le traitement. La membrane cytoplasmique a été perméabilisée pour 4 heures après avoir été exposée au plasma, et s'est refermée en moins de 24 heures. Les applications biomédicales envisagées pour l'APGD-*t* sont l'enlèvement local de tissus et l'injection d'ADN et d'ARN pour des fins de thérapie génétique.

Dans une seconde série d'expériences, une surface de polystyrène a été modifiée avec l'APGD-*t* pour faciliter l'adhésion cellulaire. L'application du plasma sur cette surface a diminué l'angle de contact de cette dernière de 93° à 35°, probablement en raison de l'incorporation de groupes polaires tels que l'oxygène et l'azote. La largeur de la surface ainsi modifiée a été déterminée en visualisant la quantité de cellules HAAE-1 ayant adhéré à la surface. La largeur de la bande de cellules ayant adhéré correspondait au double du diamètre du jet de plasma. L'utilisation de l'APGD-*t* pourrait faciliter le micro-gravure de surface par l'élimination des masques et produits chimiques utilisés en photolithographie.

Acknowledgements

First off, I'd like to thank my two co-captains, Prof. Sylvain Coulombe and Prof. Richard Leask, for their guidance and support as we ventured into new territory. I am especially grateful for the wonderful work atmosphere they have created through their enthusiastic and level-headed leadership.

I would like to express my gratitude to Valérie Léveillé, my lab mentor, for her cheerful answers to my 1001 questions, and the members of both lab groups, for their advice and friendly company. You couldn't ask for a better officemate than Nadine El-Mallah, and I thank her for always keeping a sunny outlook on life.

I owe a special thanks to the following people for their technical knowledge: Frank Caporuscio, who cut and soldered the tiny capillary over and over again, Luciano Cusmich, for making sure I didn't electrocute myself, Alain Gagnon and his team in the machine shop for building the equipment, and Ranjan Roy for keeping me out of jail.

Finally, I'd like to acknowledge the following funding sources for their commitment to the project and keeping me above the poverty line: the National Science and Engineering Research Council of Canada (NSERC), the Eugenie Ulmer Lamothe Scholarship, Fonds québécois de la recherche sur la nature et les technologies (FQRNT) and the McGill Dawson Fund.

Table of contents

List of figures

List of tables

List of abbreviations

APGD-*t*	Atmospheric pressure glow discharge torch
AC	Alternating current
BGPS	Bacterial grade polystyrene
CAM	Cell adhesion molecule
DC	Direct current
DMSO	Dimethyl sulfoxide
HAAE-1	Human abdominal aortic endothelial (cell)
HepG2	Type of human liver cell, hepatocellular carcinoma
MTT	3-[4,5-dimethylthiazol-2-yl]-2,5 diphenyltetrazolium bromide
OES	Optical emission spectroscopy
PBS	Phosphate buffered solution
PI	Propidium iodide
PS	Polystyrene
ROS	Reactive oxygen species
RNS	Reactive nitrogen species
UV	Ultraviolet

1 Introduction

There is a growing interest in the use of non-thermal plasmas in biomedicine. Non-thermal, atmospheric pressure plasma sources are particularly suitable for use with heat-sensitive substrates. Having the bulk temperature of the plasma close to room temperature reduces the negative effects of thermal loads on such materials as human tissue. At the same time, it is possible to take advantage of the highly reactive nature of the plasma to remove cells or tissue, or to deliver chemical compounds to a specific area. As the lifetime of the reactive species is small (ns – ms), the penetration depth is expected to be quite low. Therefore potential medical applications include tissue removal, surface pigmentation and skin resurfacing. There are already a few plasma devices on the medical market being used for electrocoagulation, skin regeneration, and ear, nose and throat surgery, however these devices use heat as the primary active component and not the reactive species.

At the cellular level, there are many groups investigating plasma sterilization in the laboratory. Bacterial spores can be killed after exposure to plasma due to UV radiation, charged species and reactive neutrals. The reactive species work to etch the cell until the cell membrane ruptures, and the UV radiation damages the DNA. Plasmas have been used in the medical community to sterilize instruments and devices for about a decade [1]. The specific effects of plasma on mammalian cells and tissue, however, has only begun to be investigated [2-5].

An atmospheric pressure plasma source has been developed at McGill University for use on cells and tissue [6]. The atmospheric pressure glow discharge plasma torch (APGD-*t*) is capable of very precise treatment, with a nozzle diameter as small as 150 μm, or approximately 8 mammalian cells across, assuming an average diameter of 10-30 μm. There is also a second configuration of the APGD-*t* that has a nozzle diameter of 500 μm, but is otherwise physically identical. The temperature can be kept under 40°C, eliminating any thermal damage to the tissue, while the novel design allows reactive species with a high breakdown voltage to be introduced into the plasma jet without quenching it. The

ability to deliver a variety of chemical compounds to the treated surface increases the versatility of the torch.

This thesis investigates the interactions of the APGD-*t* with biological substrates. Cell removal would be the main objective of future biomedical applications. The cells could then be discarded or used for pathological diagnoses. In a laboratory setting, the plasma torch could be used to remove a small group of cells from a culture to analyze their gene expression or metabolic function. It could act as a miniature biopsy tool, with minimal thermal damage to the cell.

Non-thermal plasma can also be used to change the surface properties of a material, without affecting the bulk properties. The non-thermal nature of the torch is also favourable for the treatment of heat-sensitive biodegradable polymers used in the construction of biomedical devices. Plasma surface modification is already widely used to prepare growth culture vessels for cell culture, where the addition of oxygen or nitrogen groups from the plasma increases the hydrophilicity of the surface, and improves cell adhesion [7].

Biological micropatterning is an emerging field in which the surface is treated to encourage cell growth within a specified matrix. It has the potential to create directed cell growth to study neuronal networks, to replicate *in-vivo* cell patterning on implants, and in biosensors. Currently, biological micropatterning is primarily done using photolithographic techniques [7]. A pattern is formed on the surface using a photoresist, UV light and a mask. The substrate is then plasma treated, and the uncovered areas become functionalized. The chemicals involved can degrade polymeric biomaterials, and the planar mask, which outlines the pattern, makes it difficult to pattern on 3-D surfaces. The small size of the APGD-*t*'s jet could be used to pattern directly onto the surface, bypassing some of the disadvantages of photolithography.

1.1 Objectives and hypotheses

The main objective of this thesis is to analyze the interactions between the APGD-*t* and biological cells. The primary goal was to investigate the effect of non-thermal plasma on a simple biological model, and to isolate the variables

responsible for any observed effects. Based on previous studies, we originally hypothesized that:

1. The APGD-*t* could be used to locally detach cultured cells
2. The detached cells would remain viable

During the experimentation, the possibility of cell reattachment was also investigated.

In a separate set of experiments, the APGD-*t* was used to functionalize bacterial grade polystyrene Petri dishes, as determined by a change in the contact angle, an increase in oxygen and nitrogen species on the surface, and an improvement in cell adhesion. The objective was to show the torch's ability to create a narrow cell track, to improve its prospects for use as a micropatterning tool. It was hypothesized that the plasma torch would enhance cell attachment to the surface by increasing the oxygen and nitrogen groups on the surface, which would also result in a decrease in the contact angle.

2 Literature review

2.1 Introduction to plasmas

There are three commonly thought of states of matter: solid, liquid and gas. On a molecular level, the difference between these three states is the amount of movement available to the molecules, the solid being the most condensed and organized state. If energy is applied to a gas, outer shell electrons are removed from the atoms, creating an electrically conductive gas, a plasma. Similar to natural plasmas which are formed using thermal energy (ie. stars) or electromagnetic fields (ie. lighting, aurora borealis), man-made plasmas are formed by applying an electric potential difference between two electrodes separated by a gaseous gap that is large enough to ionize the species found between the electrodes. This causes the breakdown of the otherwise insulating medium. A plasma can also be formed by the resistive heating of an inter-electrode gap containing a gas.

The two general types of plasmas are termed equilibrium (thermal) and non-equilibrium (non-thermal or cold). In the thermal plasma, the temperature of the heavy species is essentially equal to the temperature of the electrons, while the non-thermal plasma has its heavy species at a much lower temperature than its electrons. [8] The hot plasma is a high-density source of enthalpy and thus, finds most of its applications in the treatment of materials which require a high energy input (i.e. melting and vaporization, chemical synthesis and decomposition, spraying). The temperature of the man-made thermal plasmas ranges from 5 000 to 30 000 K, and these are typically operated at or near atmospheric pressure. The electrical energy is generated through various means including DC and low-frequency AC electrical excitation when electrodes are used, and radio-frequency excitation when coil (inductor) or parallel plate (capacitor) electrode geometries are used.

With the non-thermal plasma, the excitation and operating conditions are chosen to favor a departure between the heavy species and electron temperatures. In fact, the non-thermal plasma hosts two gases, the electron gas at a high temperature and the heavy species at a much lower temperature. This imbalance leads to considerably distinct features: since the electrons control the rates of reaction while the heavy species control the rate of thermal energy transport, the cold plasma offers a medium of high chemical reactivity with a low thermal load. Similar to thermal plasmas, non-thermal plasmas can be sustained under direct current (DC), audio-frequency alternating current (AC), radiofrequency (RF) and microwave (MW) excitations. Historically, they were produced under a vacuum in order to provide the conditions leading to the non-equilibrium state; that is, conditions providing long collision mean free paths so as to reduce the collision rates and momentum exchange rates. The temperature of the heavy species can range from room temperature to a few hundred degrees Celsius while maintaining an electron temperature of up to 5 eV (58000 K) [9]. As it is the heavy species that give the plasma its bulk temperature, cold plasmas can be used on temperature sensitive materials.

Atmospheric pressure non-thermal plasma generation has been known to exist since 1933, when Von Engle produced a glow discharge in air and hydrogen [10]. Problems including an unstable glow-to-arc transition, cooled cathodes and vacuum starting conditions were not remedied until the late 1980's. Atmospheric pressure plasmas of useful size require high breakdown and sustaining voltages, resulting in higher bulk temperatures and reduced volume plasma chambers. Various configurations were used to obtain a stable discharge at low temperatures, such as the dielectric barrier discharge (DBD), corona discharge and inductively coupled discharge [11].

The atmospheric pressure plasma jet (APPJ) is a relatively new type of non-thermal plasma that has been developed for such areas as materials processing (semiconductors), chemical analysis and sterilization. It consists of two coaxial electrodes between which gas flows. Power, generally microwave or radiofrequency, is applied to the inner electrode, and the plasma ignites once the breakdown voltage is exceeded. The gas flow carries the reactive species downstream from the electrodes, creating a plasma jet. Plasma treatment of the desired surface occurs through remote exposure (ie. the surface is not directly exposed to the active plasma but rather, to the afterglow or the recombining plasma). This reduces the damage to the substrate from charged particles and UV photons, and treatment is expected to occur due to the reactive neutral species present, increasing the chemical selectivity of the process. The distance also minimizes any effect that the electric field, which is formed between the two electrodes, might have on the substrate.

2.2 Current applications in medicine

There are a few plasma devices already being marketed to the medical community. They are mainly geared towards blood clotting, tissue removal and skin regeneration, and rely on the thermal load and electrical properties of the plasma device for treatment – not the reactive species. Lower temperature plasma treatment with the APGD-*t*, if effective, could reduce the level of discomfort felt during and after the present treatments.

Argon Plasma Coagulation (APC) was developed as an electrocoagulation device. It uses argon as the plasma forming gas, and transfers an electric current to the blood to heat the area and cause the blood to clot. When applied to biological tissue, the plasma desiccates the area during treatment, increasing the resistance of the treated area and eventually stopping the current flow. The maximum treatment depth is 4 mm, and the power ranges from 1-100 W. The temperature of the substrate must reach 50°C before coagulation begins [12]. Using an output power of 60 W, the APC has been used under anaesthesia to remove warts that had spread over a patient's heal. The treated area formed a crust and had pus and serum appearing for 1 week before healing with minimal or no scarring.

The Coblation® (ArthroCare ENT) technology is used to 'dissolve' tissue. Monopolar and bipolar devices are used so the current doesn't have to flow through the patient. A saline solution is placed over the area to be treated, and a power level of 100 W is applied, creating gas/plasma bubbles around the electrodes. OH radicals have been observed at the tip of the device, and are suspected to play a part in the remodeling of collagen during skin rejuvenation [13, 14]. Wrinkles are removed by ablating the skin's surface and restructuring the collagen supports in the dermis. The first pass removes the epidermis, while the second pass penetrates 50 μm into the dermis [15]. Applying heat (or reactive species) will denature the collagen layer, shrinking it and forming a new, smoother crosslinked layer, and eliminating some of the natural folds in the skin. The operating temperature during Coblation® treatment is between 40°C and 70°C [16], which in itself could cause the collagen to denature [17]. This technology is also being used for ear, nose and throat surgery, including tonsillectomies. Clinical studies are divided over whether Coblation® increases the risk of hemorrhaging [18, 19], or decreases post-operative pain compared with conventional techniques [20, 21]

Portrait® PSR (Rhytec) is a device that uses the thermal energy of the plasma to rejuvenate the skin. Nitrogen is used as the plasma forming gas, and the heat is used to denature and remodel collagen in the skin to remove wrinkles,

and encourage new growth in the epidermis. It provides an advantage over CO_2 lasers as the heat transfer is not chromophore dependent, and will spread evenly in the tissue [22].

2.3 Current devices in the laboratory

There are a few devices that have been designed in the laboratory for cell treatment and eventual biomedical applications. By far the most prominent is the plasma needle, shown in Figure 1, and developed at Eindhoven University by Eva Stoffels and her group [2]. The plasma needle consists of a 0.3 mm diameter metal alloy pin confined in a Perspex tube (4 mm inner diameter). Helium typically flows through the tube at a rate of 2 L/min while the plasma power ranges from a few mW to 100 mW. For experiments with cell cultures, the metal pin is confined inside a box big enough to hold the cells, and a helium environment is created within the entire enclosure. The convective force of the helium flow on the cells is minimized, but the experimental set-up is not a realistic representation of future medical procedures. It is also unknown if the exposure of the cells to a helium environment causes any disruption to their metabolism or gene expression. A RF signal (13.56 MHz) is used, and a typical voltage of 250 V_{rms} is applied to the pin. A 1 mm glow discharge is formed at the tip of the pin, and the glow extends to 2 mm as it is brought in close proximity to a conductive substrate, which acts as the ground of the circuit [2]. The Stoffels group is using the torch to treat mammalian cells [2, 3, 23, 24] and to disinfect bacterial colonies for eventual applications in dentistry [25-27]. The temperature of the plasma is kept below 37°C to eliminate any thermal damage to the cells. The hydrodynamics of the jet have been modeled [28] to explain certain geometric particularities in the bacterial killing profiles.

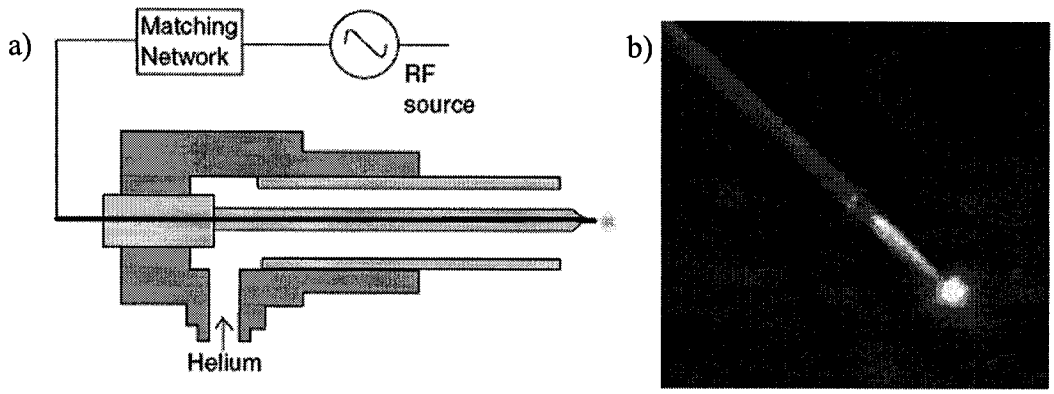

Figure 1. Schematic of Stoffels' plasma needle in a Perspex tube (a) [29], and photograph of the glow at the tip of the needle (b) [2].

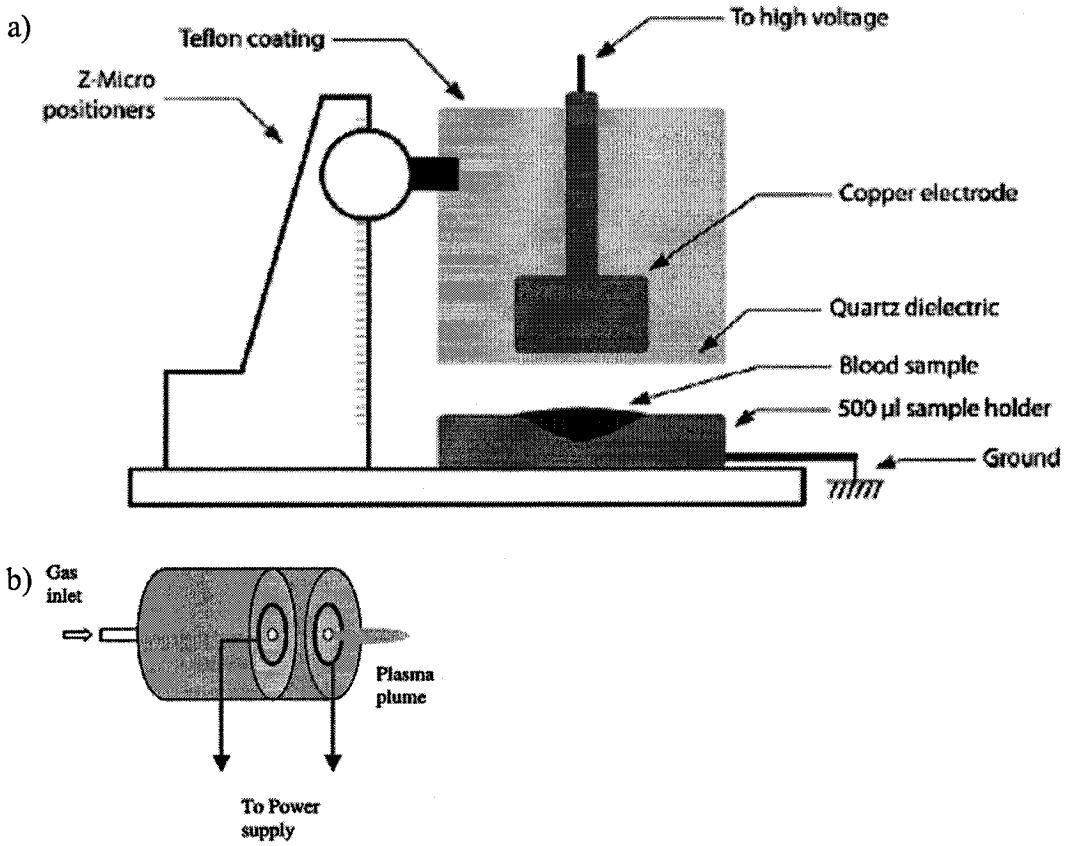

Figure 2. Schematics of the laboratory prototypes of Fridman's floating electrode dielectric barrier discharge (a) [4] and Laroussi's plasma plume (b) [30], both developed for biomedical applications.

Two other plasma sources designed for use on biological substrates were designed by Fridman [4] and Laroussi [30], which can be seen in Figures 2a and

2b respectively. Fridman's floating electrode DBD uses the treated substrate as a ground, and is being investigated as a portable device for blood coagulation and wound sterilization. Laroussi's plasma plume has a cylindrical copper ring fitted between two glass disks as the powered electrode. A 3 mm diameter hole is cut axially through the inner glass disk, through which helium flows. A plasma jet up to 5 cm long can be generated. This device has not yet been tested with a biological system.

2.3.1 Design of APGD-t

A miniature atmospheric pressure glow discharge torch (the so-called APGD-*t*) was developed at McGill University by Valérie Léveillé and Sylvain Coulombe [6], improving on the design of existing APPJs. The torch is configured for precise bio-applications, and can create a plasma jet with a diameter of only 150 μm. Helium is used as a plasma forming gas, and a capillary tube that is used as the powered, inner electrode can deliver reactive species directly to the nozzle exit. These species are ionized through collisions with the already excited helium species, and allows the addition of reactive species with minimal effects on the electrical properties of the torch (ie. breakdown voltage, stability). The gas flow pushes the plasma species out of the annulus, creating a jet. Presently, oxygen is being used as the source of reactive species. A jet of 1.5 mm can be created at a temperature of 40°C, appropriate for short exposure times on cells without causing thermal damage. Table 1 outlines the time necessary to incur a second degree burn from water at certain temperatures. Although this is not an accurate prediction of the burn time caused by the plasma jet due to the difference in heat transfer coefficients, it gives a benchmark for a desirable plasma jet temperature, and could be pertinent if a saline gel were applied to the treated area.

Table 1. Exposure time required for a second degree burn in adults when exposed to water at a given temperature [31].

Temperature (°C)	Exposure time
44	6 h
49	9 min
51	2-6 min
52	2 min
55	20-30 s
60	5-6 s
66	2 s
70	1 s

The chemical composition of the plasma jet has been examined using optical emission spectroscopy (OES) [6, 32]. This technique measures the light emission of species as they undergo a transition from an excited state to a lower state over wavelengths from 250 - 800 nm. The emission lines present in the spectrum correlate with a specific transition of a specific species, and the light intensity can be measured with respect to variables such as power level, duty cycle of the electrical excitation, and concentration of oxygen. Figure 3 shows the peak intensities of various species down the centre axis of the plasma jet. At the APGD-*t*'s nozzle exit, excited He and O are abundant. Moving down the centre axis of the jet, the oxygen and helium intensities decrease, and the N_2, N_2^+ and OH lines become stronger, likely due to the entrainment of moist air [6].

Unfortunately, not all reactive species emit light which can be measured using OES. For instance, singlet oxygen, ozone and the helium metastable atom do not have strong emission bands in the visible or do not emit at all, but are suspected to be present in the plasma jet. Ozone can be detected through light emission; an Ar-Hg lamp which has an emission line (HgI: 254 nm) falling in one of the absorption bands of ozone can be used to excite ozone, and the change in absorbance gives a representation of the quantity of ozone produced. More sophisticated techniques such as laser-induced fluorescence (LIF) can be used as well. In LIF, excited states are selectively populated with a laser pulse and the emission from the decaying excited species is collected with a sensitive photon collectors (CCD or photomultiplier tube). The hydroxyl radical (OH) and metastable helium atom can be measured relatively easily with this technique.

However, as with all efforts to quantify the miniature jet, the low levels of species produced and the optics required to focus the laser beam on the plasma source present a big challenge in obtaining accurate and meaningful data.

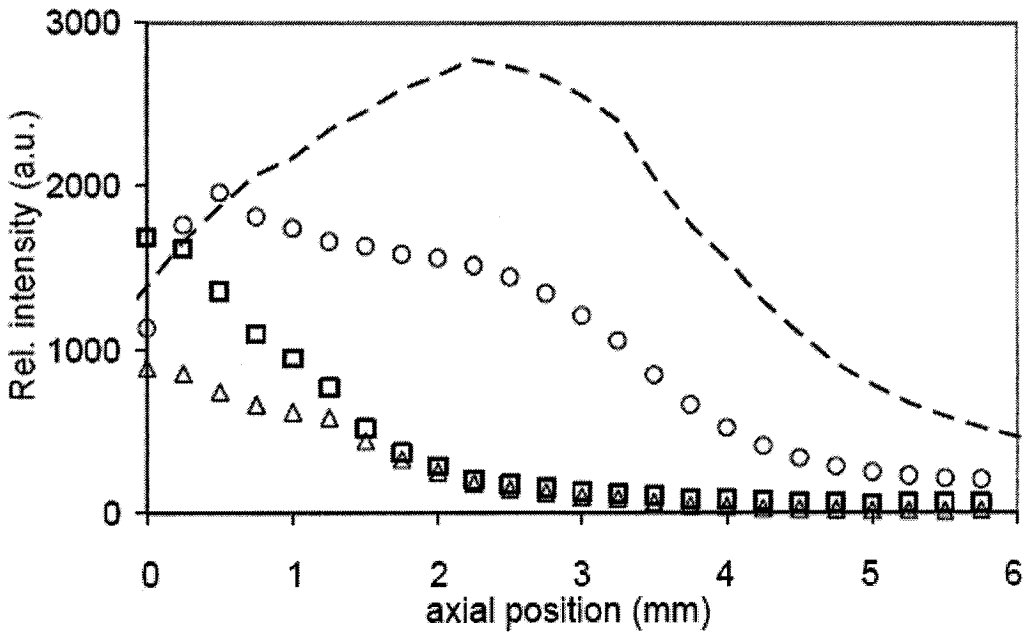

Figure 3. Axial profile of the peak intensities of selected lines at P_T ~1 W and gas flows of 1 L/min He with 10 sccm O_2 in the capillary electrode: N_2 (--) at 337 nm, N_2^+(o) at 391 nm, He (□) at 587 nm and H_α (Δ) at 656 nm [6].

2.4 Select mammalian cell biology

To get a more appreciable view of the biological scope of the project, an overview of certain cell components is required. Due to the short lifetime of the hydroxyl radical, a highly oxidative agent observed in the APGD-*t*'s jet, potential etching reactions are likely to be limited to the exterior of the cell. Therefore, the structure of the cell membrane, as well as adhesion junctions formed between cells and the extracellular matrix will be described. Singlet oxygen and molecular oxygen have longer lifetimes and could potentially diffuse into the cell, however apoptotic pathways resulting from an imbalance of chemical species will not be discussed. A summary of significant ROS in biology, their lifetimes and potential reactions is given in Table 2.

Table 2. A summary of significant ROS in biology.

Species	Lifetime	Radius of diffusion	Potential reactions with cell	Detected in jet?
OH	2 ns	20-30 Å [33]	• Most reactive ROS • Reacts with many organic molecules ie. phospholipids, DNA	Yes
Singlet oxygen	3.8 μs in water [34]	0.7 μm [a] [35]	• Increases propagation rate of lipid peroxidation • Induces cytotoxicity in photosensitizing reactions	Suspected
Ozone	70 ns in lipid bilayer [36]	100 Å	• Oxidizes membrane lipids and proteins • Reacts with biomolecules to form singlet oxygen	Suspected
$O_2^{\bullet-}$	100 μs [37]	0.7 μm [b]	• No direct effect on proteins/lipids • Reacts with NO• to give $ONOO^-$ • Generated *in-vivo* in cells	No

[a] radius of diffusion in a cell

[b] calculated using $r = (6Dt)^{1/2}$, with $D \sim 1 \times 10^{-9}$ m^2/s for small radicals in water [38]

2.4.1 Structure of the cell membrane

The plasma membrane allows nutrients and waste to travel to and from the cell, while maintaining the structural integrity of the cell and sensing changes in the external environment. It is made up of a lipid bilayer and proteins, each accounting for about 50% of the weight of the membrane. The lipids form the basic structure, while the proteins distributed throughout the membrane are responsible for cell communication, recognition and adhesion. The lipid bilayer is arranged with the hydrophilic heads facing out, and the hydrophobic tails forming the interior of the wall. The long chain hydrocarbon tails contain polyunsaturated fatty acids (PUFAs), whose double bond is an easy target for the abstraction of a hydrogen atom (Figure 4). The chain length and composition of the phospholipids, and the amount of cholesterol affects the fluidity of the membrane [39].

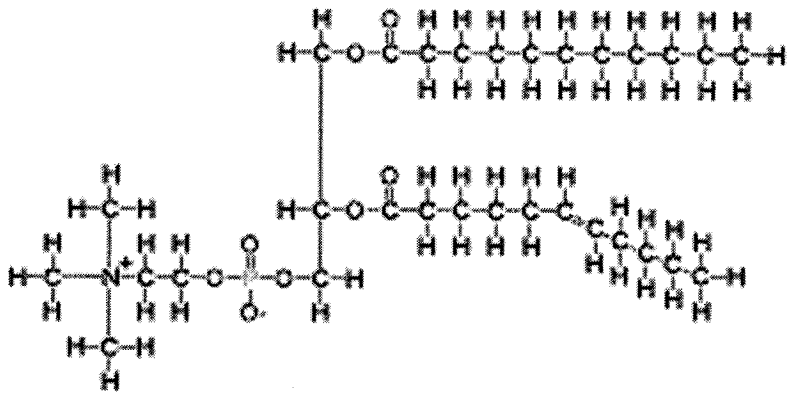

Figure 4. Molecular structure of a phospholipid. The double bond on the hydrocarbon chain is targeted by the hydroxyl radical, initiating lipid peroxidation [40].

2.4.2 Cell adhesion

There are two types of anchoring junctions between mammalian cells that are primarily responsible for cell-cell and cell-matrix adhesion: adherens and desmosomes or hemidesmosomes (figure 5a). They firmly link the cells to each other or to the extracellular matrix, and are predominantly found in areas of high mechanical stress like the skin epithelium or cardiac muscle [39, 41]. Cell adhesion is an active process – the cell must express the required proteins to adhere, and dead cells will detach and float in the media.

Within the cell, adherens junctions connect the actin filaments (a component of the cytoskeleton) of the cell to exterior bonding sites. Cell-cell adherens are configured as a belt around the entire cell (zonula adherens), while cell-matrix adherens are formed in little spots called focal contacts or adhesion plaques.

Desmosomes and hemidesmosomes bind to intermediary filaments of the cell such as keratin in epithelial cells. Patches of dense plaques of intermediary filaments are formed on the inside of the cell, providing a strong base to which the adhesion proteins can bind. They transfer shear stresses between cells, improving the strength of the whole cell layer. Desmosomes form cell-cell adhesion

junctions, whereas hemidesmosomes bind the cell to the extracellular matrix (ECM).

Both adherens and desmosomes rely on transmembrane glycoproteins (proteins with carbohydrates on the end) to pass through the cell membrane and mediate cell adhesion. The two main cell adhesion molecules (CAMs) involved in these junctions are cadherins (cell-cell adhesion) and integrins (cell-matrix adhesion). There are more than 100 different cadherins, each responsible for separate homophilic interactions. Classical cadherins are the most widely expressed, and include type E- (epithelial cells), N- (nerve, heart and lens cells), and P- (placenta and epidermis) cadherins. Figure 5b shows how cadherins form adherens junctions by passing once through the cell membrane and binding to the catenins, which connect the cadherins with the actin filaments. Another class of cadherins is the desmosomal cadherin, which interact with plankoglobin and plankophilin to connect to the intermediary filaments.

Integrins are heterodimers that mediate heterophilic interactions. Each integrin is composed of an α and a β subunit, of which there are 18 and 8 known units in mammalian cells, respectively (Figure 5c). The 24 combinations of subunits bind with specific ligands in the ECM. For instance, $\alpha 2\beta 1$, $\alpha 6\beta 4$ and $\alpha v\beta 5$ are expressed by keratinocytes in the epidermis, and are receptors for collagen, laminin and vitronectin, respectively. Interestingly, the $\alpha 5\beta 1$ integrin (fibronectin receptor) is only expressed in cultured keratinocytes [42]. Integrins are the main CAM in cell-matrix adherens junctions, as well as hemidesmosomes.

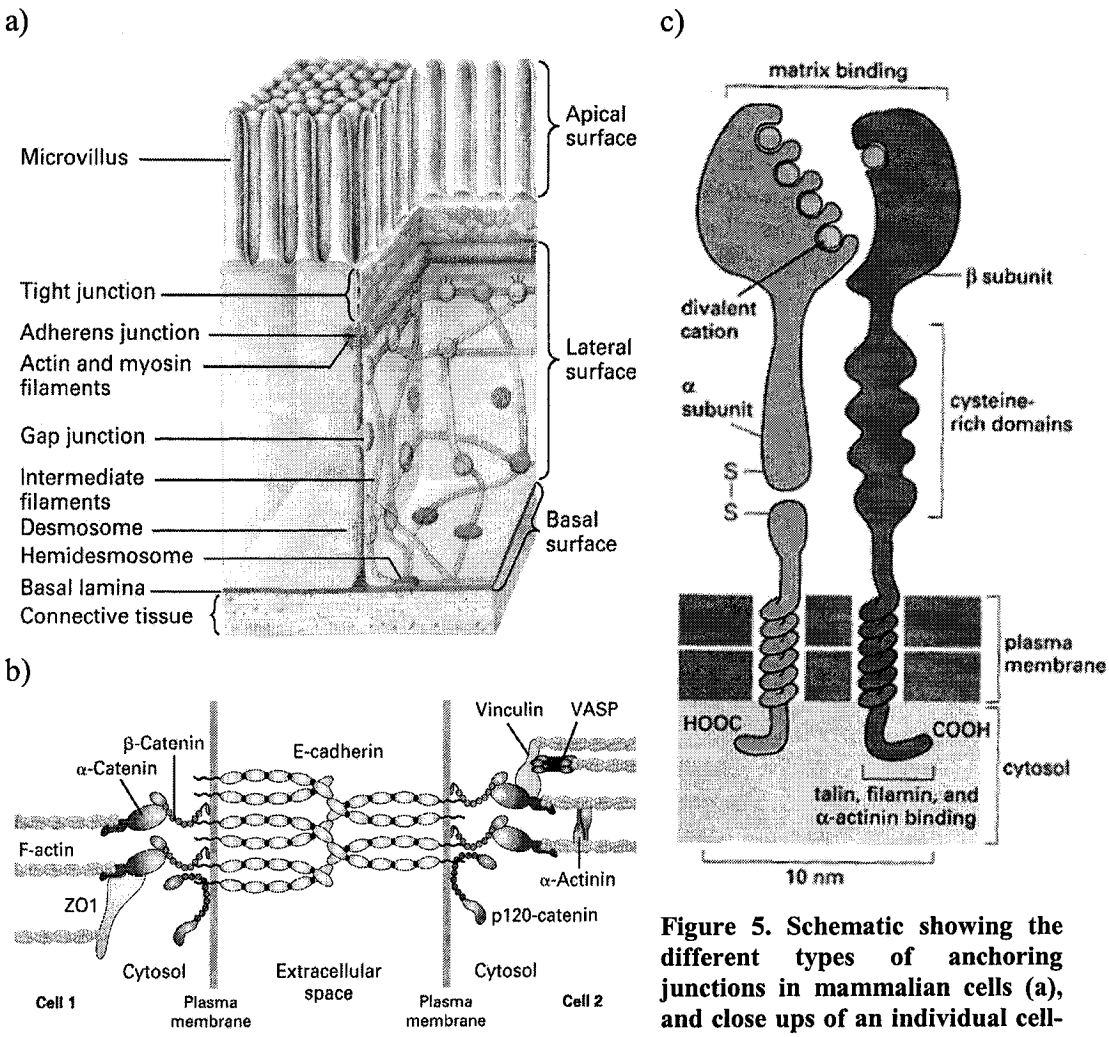

Figure 5. Schematic showing the different types of anchoring junctions in mammalian cells (a), and close ups of an individual cell-cell bond (b) and an integrin (c) responsible for cell-matrix binding [41, 43].

There are two final types of CAMs – the immunoglobulin (Ig) superfamily and selectins. IgCAMs use the Ig domain (antibody) to interact with antigens, and are found in neurons, endothelial cells and tight junctions. Selectins use the Ca^{2+}-dependent lectin domain to help the immune response of white blood cells, allowing them to bind to inflammation sites and foreign invaders.

The strength of anchoring junctions relies on many relatively weak interactions between transmembrane adhesion proteins, forming a strong overall bond. As integrins and cadherins are calcium-dependent proteins, a Ca^{2+} deficiency can result in blistering (integrins no longer bind cells to basement membrane).

2.5 Plasma and biology at the cellular level

2.5.1 Plasma sterilization

The interaction of a plasma with living organisms has been most widely studied in relation to plasma sterilization. Traditional sterilizing processes use heat and dangerous chemicals to denature the chemical structure (T>126°C), destroy proteins to disrupt the metabolic pathway, etch the cell membrane, inhibit oxygen or other energy-releasing metabolites, and withhold key nutrients to starve the cell [44]. During plasma sterilization, the reactive species, UV, and charged particles of the plasma are used to deactivate all microorganisms present. The application of these studies has been focused on the sterilization of medical devices, food, and environmental discharges [45], although the premise of causing cell death transfers to biomedical treatments.

To assess the level of sterilization, various techniques are used. By far the most common method to test for cell death is staining. Should the cell membrane rupture, the stain will react with one or more of the contents of the cell, colouring its contents. Intact, living cells will continue to remain colourless, or will be stained a different colour depending upon the stain used. Other methods that recognize a change in cell function upon death are laser-induced fluorescence [46, 47], or the measure of the change in current passing through a single cell [48], although the outcome of these techniques are not as easily interpretable as staining.

2.5.1.1 Sterilization parameters

Plasma parameters that influence the killing efficiency can be roughly divided into internal plasma operational variables, and external species variables. Some of the more important factors in atmospheric plasma sterilization that can be controlled on the APGD-*t* are discussed below [49].

Gas composition – Directly related to the type of reactive species and charged molecules that are available in the plasma, as well as the intensity and wavelength

of UV emission. Herrmann *et al.* [45] (and references thereof) demonstrated with his atmospheric pressure plasma jet that the addition of oxygen to helium decreases the D-value (time required to kill 90% of population) over plasma treatment with just helium, most likely due to the ozone, atomic and singlet oxygen species formed in the plasma. By adding CF_4 to an oxygen rich stream, a higher concentration of oxygen atoms can be achieved, and the fluorine atoms will remove hydrogen atoms from the surface, leaving a reactive layer that is more easily etched.

Hydrogen peroxide (H_2O_2) has also shown itself effective for sterilization, however it is an anti-bacterial agent on its own. Its success in the commercially available Sterrad® plasma sterilizer has been credited to the peroxide liquid phase, with the plasma phase removing harmful residues that are leftover.

Kuzmichev *et al.* [45] (and references thereof) reported that optimal germicidal properties were achieved using moistened oxygen and air. The OH radical is expected to attack the outer layers of the cell, while NO and NO_x improve the lethality of the process [45].

Gas flow – Increasing gas flow increases the rate of generation of reactive species, or at least enhances the transport of reactive species to a remote substrate. It is expected that the killing efficacy will reach a maximum value once there is an excess of reactive species that can be used effectively, or once the residence time of the reactive species is too short for treatment.

Power – Increasing the plasma power leads to a higher electron density and consequently, more reactive species are produced.

Microorganism – The resistance to the plasma depends on the type and distribution of microorganism being treated. The strain and method of preparation of the microorganism are shown to affect the parameters required for sterilization, therefore it is recommended that commercial products be used to reduce variability.

Substrate – The substrate used can influence the D-value of microorganisms. Montie *et al.* [10] treated *E. coli* placed on various substrates and found that cell death occurred the quickest on a polypropylene backing (D = 6 s), followed by glass (D = 33 s) and agar (D = 70 s). The surface roughness and porosity of the substrate are assumed to play key roles in the geometry and exposure of the cells.

Temperature – It is suspected that temperature influences the killing mechanism. Hury *et al.* [49] (and references thereof) observed that the killing efficiency did not necessarily decrease with a drop in temperature. The efficiency was greatest at 60°C, followed by -15°C and then 15°C. By Arrhenius' law, the etch rate increases with temperature:

$$R = Ae^{\frac{-E_a}{kNT}} \qquad (1)$$

Where R is the etch rate [s^{-1}], E_a the activation energy [kJ/mol], k is Boltzmann's constant [kJ/K], N is Avogadro's number [mol^{-1}] and T the temperature [K]. The improved sterilization at -15°C over 15°C is thought to be due to the hypersensitivity of spores to UV when frozen.

Other factors to be aware of and that influence the germicidal effect of the plasma, but are not variables in the current project, are pressure, excitation frequency, exposure type (direct or remote) and spore packaging.

2.5.1.2 Mechanisms of cell death

The mechanisms leading to cell death due to an atmospheric plasma source are not yet fully understood. The three proposed agents that contribute to cell necrosis are UV radiation, reactive species and charged particles, although the relative contribution of each of these factors varies with the plasma parameters mentioned above.

Reactive species formed in the plasma are suspected to be the main cause of cell death. The reactive species mentioned above, including atomic oxygen,

singlet oxygen, ozone, OH and $NO^{\cdot}$ radicals all react with the cell. The oxidation of the lipid membrane to form unsaturated fatty acid peroxides releases CO_2 and H_2O, and its eventual rupture is the end result. The broken membrane allows the cytoplasm and cell organelles to leak into the surrounding environment (Figure 6) [2, 10, 45, 50]. Other cell components affected by reactive oxygen species include the proteins, whose amino acids are oxidized, and DNA [10]. Ozone is also known to inhibit cellular respiration [45].

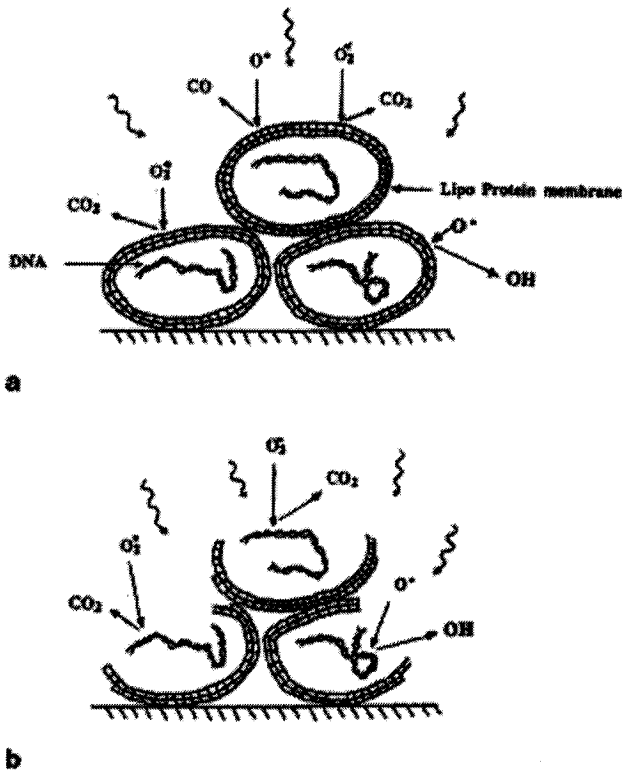

Figure 6. The expected effect of the reactive oxygen species from plasma on the cell membrane [50].

UV irradiation has been proven to damage cells by attacking the DNA [45]. Cells have a high UV absorption coefficient, therefore UV radiation of tissue will kill the top layer but won't penetrate into deeper layers. The contribution of UV irradiation to cell death from atmospheric plasma sources, however, has been shown to be minimal. Kelly-Wintenberg *et al.* [51] used a conventional heat-sealed medical sterilization bag to separate the effect of reactive oxygen species (ROS) and UV. The bag was intended to allow ethylene oxide, and hence ROS to penetrate while blocking most of the UV. *Staphylococcus*

aureus exposed to the plasma inside and outside of the bag had similar sterilization efficacies. It was concluded that there was no difference in the killing efficacy of the plasma on openly exposed bacteria relative to bacteria placed inside the bag. UV likely does not play a major role in atmospheric pressure plasma sterilization as there is not enough intensity in the "germicidal range" of 220 nm to 280 nm [45].

The third perpetrator in cell death is charged particles. On irregular cell surfaces, the charge density can create an electrostatic force which overpowers the tensile strength of the membrane, causing it to burst. Laroussi *et al.* [9] exposed both Gram positive and Gram negative bacteria to a 97% He/3% O_2 resistive barrier discharge atmospheric plasma, and observed that the cell membrane of the Gram negative (*E. coli*) strain was destroyed, while no morphological changes were apparent in the *Bacillus subtilis* Gram positive bacteria. Gram negative bacteria are characterized by thin cell membranes and an irregular outer layer, while gram positive contain a thicker, smoother membrane reinforced with a murein layer. Charged particles are not expected to play an important role in remote exposure systems (where the plasma particles are created and then put in contact with the surface by convection), and can be neglected in APPJ set-ups [45].

Therefore, the main mechanism of cell death using non-thermal, atmospheric pressure plasmas is oxidation of cell components by the reactive species in the plasma jet.

2.5.2 Non-fatal plasma treatment of mammalian cells

Prior to cell necrosis, interesting changes to cell metabolism have been observed. Although the health of removed cells after plasma treatment is not generally a concern, the consequences of low levels of plasma treatment does provide more insight into the mechanism with which the plasma acts to kill and deactivate the cell. Maintaining cell viability after plasma treatment could also be a useful tool for biopsies, to remove small samples of living cells and to insert specific markers into a cell.

Stoffels *et al.* [2] found that cell necrosis occurs in Chinese hamster ovarian cells when treated by the plasma needle operating at 0.2 W for 10 s. The plasma was created by flowing pure helium, however leakage of ambient air into the jet was expected to be between 0.5% to 1% of the gas flow. When treatment conditions were reduced to 50 mW for 1 s, the cells detached from each other, and at longer treatment times, from the substrate as well. The detachment was suspected to cause a temporary change in cell metabolism that affected cell adhesion, in particular the cadherins that binds cells together, and integrins which attach the cell to the substrate, although no specific tests were performed to confirm those suspicions. Detachment was not instantaneous, occurring up to 1 minute after treatment. The cells reattached after 2-4 hours, and after 24 hours resembled untreated samples.

The geometry of the necrotic cells, detached cells and unaffected cells were described by Kieft *et al.* [24]. The necrotic cells were found at the centre of a bulls eye, a void of detached cells encircling this, and the unaffected cells on the outer edge, corresponding to a decrease in the power level reaching the cells. In a second cell experiment that used the torch configuration rather than the confined box, the effect of liquid height during plasma treatment was investigated [3]. Cells were exposed to the plasma for 30 s, using a helium flow rate of 2 L/min through a 5 mm ID Perspex tube. They found that the void size left in the cell culture corresponded to the area covered by a very thin layer of media (< 0.1 mm) and no void was formed at higher media coverages, indicating that the penetration depth of reactive species through the media is very low. When no media was used during treatment, a necrotic zone formed in the centre of the void, presumably due to the desiccation of the cells.

The reactive species were assumed to play a key role in cell detachment, as the cells were not affected when turned upside-down with a layer of glass between then [2]. The oxygen species associated with the dissociation of H_2O_2 (OH, peroxide, hydroperoxy radicals) were also not expected to play a big role in cell removal, as UV photosensitization with H_2O_2 did not produce any cell

detachment. [23] As expected, when cells were exposed to the lethal combination of UV and H_2O_2, cell necrosis was observed.

Laroussi *et al.* [52] investigated the effect of sub-lethal plasma treatment on the heterotrophic pathway of *E. coli* cells. Plasma treated cells were placed on 95 different carbon substrates, predominantly amino acids, carbohydrates and carboxylic acids. A dye added to the substrates indicated the utilization of the particular substrate with a change in colour intensity. The consumption of each substrate was monitored relative to a control and any differences were noted. For most substrates, no difference in consumption was found between it and the control wells. There was an increase usage of L-fucose, D-sorbitol and D-galacturonic, and a decrease usage of methyl pyruvate, dextrin and D L-lactic acid relative to the controls. These were presumed to indicate changes in cellular functions such as enzyme activity.

2.5.2.1 Plasma permeabilization of the cell membrane

There is a growing interest in the ability to insert molecules into cells without causing cell death. There are a few ways to do this, including microinjection and electroporation. Microinjection uses a fine needle to mechanically insert the compound into the cell – a manual, time consuming process. Electroporation is the permeabilization of the cell membrane using an electric field. This is particularly relevant to plasma systems, which generate an electric field in the interelectrode region. The effect of the electric field in remote exposure systems still needs to be determined, although it is expected to be minimal as the field strength decreases with an increasing plasma-substrate distance

With electroporation, it is possible to transfect many cells at once, but the process works best on cells suspended in culture. Electric pulses (μs to ms range) are applied to the cell to induce a transmembrane voltage difference of approximately 1 V. Although the exact mechanism is not fully understood, it is believed that the dipole created in the cell causes the bilipid layer to temporarily rearrange, forming hydrophilic pores of at least 1 nm in diameter [53, 54]. This

allows large molecules to easily diffuse across the cell membrane. The time scale for the creation of pores is 10^{-6} s, while it takes around 1 s to reseal at room temperature.

The technology is promising for gene therapy and drug delivery, and is being used in clinical trials for electrochemotherapy. The process involves introducing an anticancer drug (ie. bleomycin) to the target area, and then electroporating the cells with a hexagonal needle configuration. This results in a vast improvement over treatment with the drug alone, or no treatment. The electroporation also reduces the amount of bleomycin needed for successful treatment by 500 to 5000 times. This localized treatment reduces the side effects normally associated with chemotherapy [55].

Cell permeabilization can also be used for gene therapy, which involves introducing foreign DNA or RNA to a cell to change its function. Viral vectors are the most common method of DNA transfection at the moment, however due the immune response, it is difficult to get reproducible results, and has a size limitation of 5 kb (1 b = 1 DNA/RNA building block). Electroporation can be used as an alternative to viral vectors, as it allows many cells to be transfected at once, and takes very little time to perform [55].

Astellas Pharma Inc. in Japan has patented a process which describes the use of plasma to transfect DNA into cells for gene therapy [56], and has published preliminary results [57, 58]. A pre-made plasma generator is used, with 100 V applied to the electrode. The electrode gap can be varied, and in experiments described in [57] is set to 3 cm, half the diameter of a Petri dish. The dish is set on a turntable so that all cells can be treated. A gas flow rate of 90 L/min flows through the electrode gap, forming a jet. The cells are placed 2.2 cm from the end of the electrodes, and are covered with a media layer 0.07 mm deep.

DNA (3.1 MDa) was added to the culture prior to plasma treatment. The transfection rate and the mortality rate were measured by flow cytometry after 24 hours, and were found to be ~20% and 2% respectively, depending on the cell type and exposure time (1-3 s). When the DNA was added 2 s, 10 s or 5 minutes after plasma treatment, the transfection rate dropped to 0%, indicating that the

pores resealed within 2 s. It was presumed that the reactive species in the plasma broke some DNA strands in the media, as the addition of DMSO, a reducing agent, inhibited this effect. They suggested that the pores formed in the media were due to the electric field and not the reactive species, as the pore kinetics were similar to electroporation.

2.6 Plasma surface modification

Plasmas are also used to alter the surface chemistry of items like textiles and semiconductors. The high energy and reactivity of a plasma can be used to modify the surface of a material, without affecting its bulk properties. For instance, the biocompatibility of the surface of a polymeric biomaterial can be altered, without affecting its compressive strength or fracture toughness. The high energy species can break chemical bonds or cleave atoms, leaving available surface sites to which other atoms, molecules or monomers can bind. Plasma surface modification is already widely used to etch semiconductors and prepare cell culture vessels.

The treatment of biomaterials with non-thermal plasmas has been widely researched, and various technologies are used commercially in the modification of tissue culture vessels. Cell attachment is enhanced by modifying the culture dish surface using plasmas of various gas compositions to increase the oxygen and/or nitrogen groups incorporated into the surface [59, 60]. The modifications reduce the hydrophobicity of the surface, and increase cell adhesion. At the laboratory level, researchers have investigated plasma treatment to micropattern surfaces to study neuronal networks [61], the fabrication of biosensors and the imitation of *in-vivo* cell patterning on implants to improve biocompatibility.

Currently, most plasma patterning is done using photolithography, outlined in Figure 7. A chemical coating is hardened with UV light through a laser-cut metal mask, and the unaffected areas are washed clean. The whole surface is plasma treated, functionalizing the areas not covered with the resist layer [7]. The resist is removed, and the functionalized pattern is left on the surface. There are a few aspects of photolithography that inhibit its use on

biomaterials. First, it has traditionally been used on glass or silicon surfaces, and the chemicals used in the process can accelerate the degradation of the polymers used as biomaterials [62] and introduce a source of contamination to the cell culture. Secondly, masks are costly, and give only one pattern. Moreover, the masking process does not work well on curved surfaces. Schröder *et al.* [63] have been successful in plasma micropatterning directly through a mask without using the chemical resist, however, they found that the mask was sensitive to handling and heat. The mask needs to be in direct contact with the surface, or else the plasma will diffuse under the mask and the borders will be ill-defined.

Chemical photoresist methods also require additional processing steps and greater use of chemicals, including sputtercoating, baking, exposure to UV light, immersion in a developing agent, and the solvent removal of the photoresist. The use of a miniature plasma source that is capable of 3-D movement could circumvent the present difficulties of micropatterning on asymmetric, biodegradable surfaces, and reduce the number of steps involved in sample preparation. By attaching the plasma torch to a robotic arm, a pattern could be created directly on the substrate.

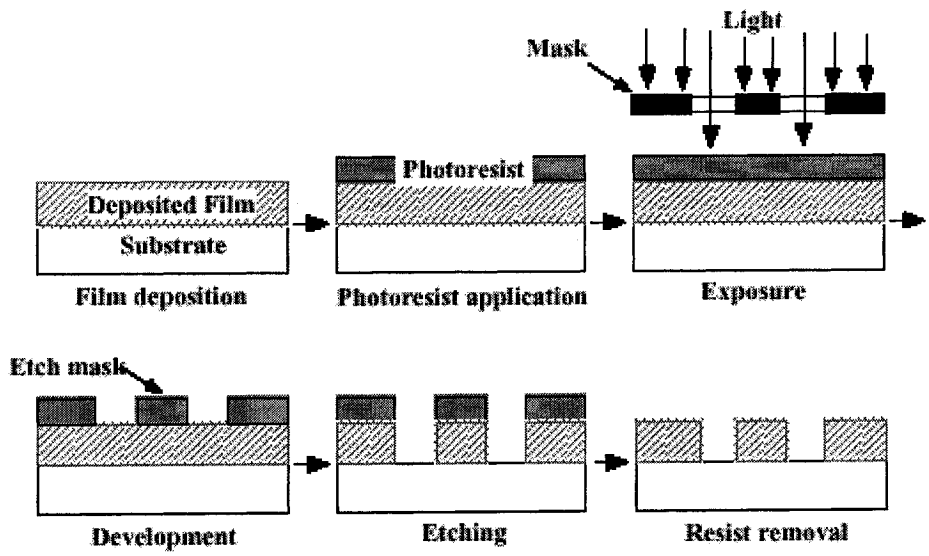

Figure 7. Flowsheet of the steps involved in patterning using photolithography [64]. Direct plasma surface patterning could eliminate the need for the photoresist (step 2) and the mask and UV light (step 3).

Important criteria in creating a successful micropattern include a small and variable spot size (<100 μm), crisp borders and no harm to the degradable polymer substrates used for biomedical devices. As a non-thermal plasma torch can operate at atmospheric pressure and room temperature, and is assumed to produce a negligible quantity of UV radiation, it should be able to process a wide variety of temperature- and UV-sensitive materials.

Identifying factors that are linked to increased cell adhesion include surface tension (hydrophobic vs. hydrophilic) and surface chemistry. These are generally measured by contact angle and x-ray photoelectron spectroscopy (XPS), respectively. Detrait *et al.* [65] used photolithographic techniques to pattern a bacterial grade polystyrene dishes (BGPS) with an oxygen plasma. The contact angle decreased from 92° to 53°, and cells were shown to adhere preferentially to the treated areas. XPS results indicated an increase of oxygen on the surface after exposure to the resin and developer used in photolithography, but no further increase after plasma treatment and a wash step [66].

In a separate approach to plasma micropatterning, various polymer substrates were functionalized with a NH_3/Ar plasma, after which select areas were passivated with a hydrogen plasma directly through a mask. The contact angle decreased on all substrates after exposure to the ammonia plasma, and increased relative to the pristine polymer after the passivation step. Cell density was also much higher on the ammonia treated areas, over the untreated and passivated polymer [63]. A small spot XPS (spot size 100 μm) was used to create a profile of the functional groups on the surface, and which was comparable to the mask pattern. The XPS data was processed to provide contrast images of the patterned surface [67].

De *et al.* [68] treated PS surfaces with a helium plasma at atmospheric pressure and also recorded a decrease in the contact angle (90° to 79°) and a slight increase in C=O and C-N groups on the surface. They accounted the change in surface chemistry to the ambient air leaking into the reactor and reacting with the reactive sites created by helium.

3 Experimental methods

3.1 The plasma torch

The construction of the miniature atmospheric pressure glow discharge torch (APGD-*t*) has been described in detail by Léveillé and Coulombe [6]. Figures 8 and 9 present a photo and schematic of the torch itself, while Figure 10 shows the complete electrical set-up required to power and control the torch. The torch consists of two concentric electrodes; the inner, powered electrode is a stainless steel capillary (I.D. = 0.1775 mm, O.D. = 0.3550 mm), and the outer grounded electrode is a silver epoxy painted over 2 cm on the exterior surface of a quartz tube (I.D. = 2 mm, O.D. = 4 mm). The quartz tube is tapered at the exit to form a converging nozzle, with two possible configurations. In the first, the nozzle terminates with an inner diameter of 500 μm, while in the second, the final inner diameter is 150 μm. The smaller diameter nozzle was only used in functionalization experiments. The tip of the capillary electrode ends ~0.5 mm upstream of the end of the nozzle. Helium is used as the plasma-forming gas and flows through the annular space between the capillary and the quartz tube at a nominal rate of 1 L/min. The gas flow carries the plasma species out of the quartz tube, creating a jet. 3 cm^3/min (0.3 $^{v}/_{v}$%) of oxygen, a source of reactive species, is injected through the capillary, as this corresponds to the maximum production of atomic oxygen species [32]. The recombination and de-excitation of helium species contribute to the excitation of oxygen from the capillary, as well as oxygen and nitrogen species from the air that diffuse into the jet. The torch is mounted on stage that allows precise positioning of the torch in all three axes.

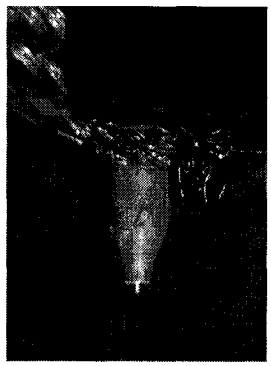

Figure 8. Close up of the 150 μm I. D. torch nozzle (painted with silver epoxy) and plasma jet.

Radiofrequency (13.56 MHz) power is generated using a waveform generator (Hewlett Packard, model HP 33120A). The amplitude of the RF carrier signal is modulated using a square wave generator (Racal Dana, model F64) and the signal amplified with a broadband RF amplifier (Amplifier Research, model 75A250). The duty cycle of the modulated signal was set to 10% to keep the power level, and hence the bulk temperature of the plasma jet, at a low level. Figure 11 shows the effect of the duty cycle on the plasma jet's power and temperature [6]. This minimum duty cycle was a constraint stemming from the equipment. The modulation frequency was set to 100 Hz.

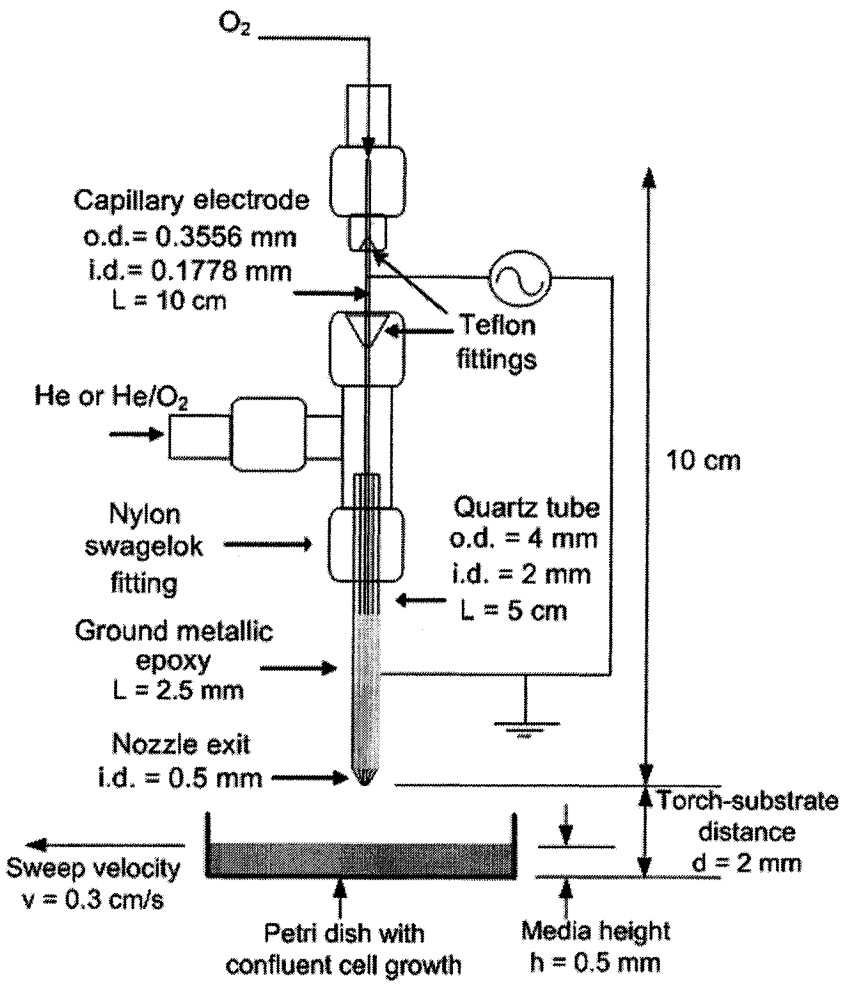

Figure 9. Schematic of the miniature plasma torch, modified from Léveillé and Coulombe [69].

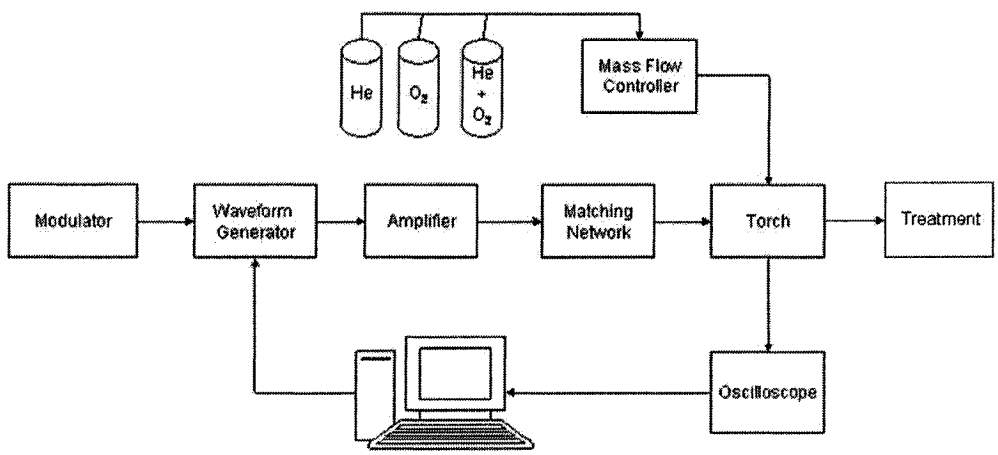

Figure 10. Schematic of the existing torch set-up.

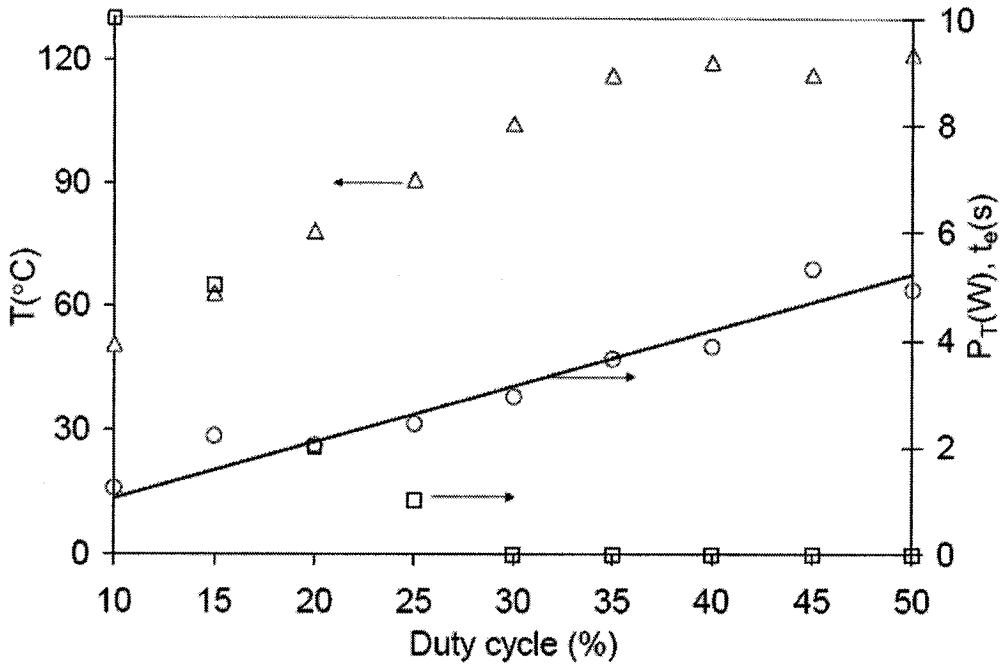

Figure 11. The effect of the duty cycle on the APGD-*t* power, P_T [W] (o), gas temperature, *T* [°C] (Δ), and exposure time to skin before feeling thermal pain, *te* [s] (□) with a helium flow rate of 1 L/min [6].

A homemade series inductor was used as an impedance matching element (L = 21 μH). The matching network ensures that the power supply sees an equal load through the circuit (ideally, 50 ohms resistive), which will allow a maximum transfer of power and the resonant circuit conditions needed to achieve a high operating voltage from a low voltage source. By adding this inductor in series with the plasma torch, this ideal load can be approached, and the reflection of power kept to a minimum. A tunable matching network (MFJ, model MFJ 969) has recently replaced the homemade one. A power meter (Rohde & Schwarz Directional Power Meter NAS) measuring the forward and reflected power levels from the amplifier generally shows very low levels of reflected power (<10%). Current and voltage probes (Tektronix, model CT-2 current transformer and model P5100 passive voltage probe) were connected to a digital oscilloscope (Tektronix, model TDS 3054B), which was used to monitor the circuit current and torch voltage waveforms. A LabView™ interface was used to control the various components of the torch set-up.

The nominal operating voltage and current on the torch were ~750 V_{ppk} and 550 mA_{ppk}, respectively, with a phase angle of around -80°. This resulted in a plasma power of ~1 W. The visual length of the jet was 1-2 mm, while its temperature ranged between 37°C and 40°C (as measured with a 0.5 mm diameter type K thermocouple at the tip of the plasma jet). The typical operating conditions are summarized in Table 3.

Table 3. Standard operating parameters of the miniature atmospheric plasma torch.

Parameter	Standard operating value
Flow He (L/min)	1
Flow O_2 (sccm)	3 (0.03 v/v%)
Current (mA)	550
Voltage (V)	750
Phase angle (°)	-80
Frequency (MHz)	13.56
Modulation frequency (Hz)	100
Duty cycle (%)	10
Power to torch (W)	~1
Forward power to tunable matching network (W)	20
Reflected power (W)	0.1
Bulk temperature (°C)	40

3.2 Optical emission spectroscopy

Optical emission spectroscopy (OES) was used to identify some of the excited species created in the plasma jet having radiative transitions in the 250 – 800 nm range. A 400 μm fibre optic cable was used to collect the light emitted from the plasma. As the fibre optic cable has an acceptance angle of 24.8° (the angle that the fibre optic cable sees), a lens (Newport, model SBX058, f = 15 cm) was used to focus a light collection spot on the plasma jet. A spacing of 30 cm was used between the jet and the lens, and the lens and the fibre optic

(enlargement of -1). A low resolution UV/VIS spectrometer (Ocean Optics, model USB2000) was connected to the fibre optic cable. The optical emission spectra were displayed using Ocean Optics' OOIBase32 software. Prior to collecting data, it was ensured that the spectrometer would not be saturated during the test by adjusting the experimental variable until a maximum emission was found. The integration time was then changed to achieve an intensity (in scope mode) of 1000 – 3000 counts. To correct for the change in sensitivity of the spectrometer over the range of wavelengths, a reference spectrum was used corresponding to the integration time for the given experiment. The background noise was eliminated by storing a dark of the experimental set-up (the plasma is turned off).

3.3 Cell culture and plasma treatment

The protocol for the plasma treatment of cells is provided in Appendix 1. All cell culture products were purchased from ATCC, unless otherwise noted. Human hepatocytes (HepG2) were cultured for plasma treatment in minimum essential medium eagle (MEME) supplemented with 10% fetal bovine serum, 100 μg/mL penicillin and 100 μg/mL streptomycin at 37 °C in a 5% CO_2 humidified incubator. Cells were expanded in T-75's, subcultured at a ratio of 1 : 2.5, with a media change after 3 days, and trypsinizing after 7 days. Cells were seeded in Corning® 60 x 15 mm tissue culture Petri dishes in preparation for plasma treatment and allowed to grow until they just reached confluence (~4-5 days). Allowing the cells to continue to grow after the culture had reached confluence made it more difficult to remove cells during plasma treatment, as the cell stack.

Human aortic endothelial cells (HAAE-1) were cultured for plasma treatment and surface functionalization experiments. These cells grow in a monolayer, and the cell borders are easy to determine. The cells were incubated at 37°C in a 5% CO_2 humidified incubator in endothelial cell growth medium (C-22010, Promocell, Germany) supplemented with 10% fetal bovine serum, 50 μg/ml gentamicin, 10% penicillin streptomycin (all from Invitrogen), and supplement mix (C-9215, Promocell, Germany: 0.4% endothelial cell growth

supplement, 0.1 ng/ml epidermal growth factor, 1 μg/ml hydrocortisone, 1 ng/ml basic fibroblast factor and 50 ng/ml amphotericin B). Late pass cells (> pass 5) were seeded at high density into 60 x 15 mm tissue culture dishes to ensure confluent cell growth. The cells were ready for plasma treatment or the analysis of surface modification experiments within 1-2 days.

During the plasma treatment of cells, the nozzle diameter of the APGD-*t* was 500 μm. Cells were taken out of the incubator, the media changed to remove any floating cells, and the operating parameters adjusted. The depth of the media covering the cells (media height, h), the distance between the nozzle exit and the substrate (d), and the linear sweep speed of the sample (v) were fine-tuned in order to achieve cell removal after plasma treatment, but not after exposure to the high gas flow which can mechanically shear the cells. The Petri dish was moved by hand under the lit torch creating a treatment path in the cells. The power to the torch was then turned off, leaving the gas flow on, and a second path was made through the cells to distinguish the effect of the gas flow alone on cell detachment.

The cells were gently rinsed with PBS (Fisher Scientific), stained with crystal violet (Beckton-Dickinson) and photographs taken of the treated areas. Separate dishes were stained with trypan blue to investigate the viability of the cells.

To ensure that the jet temperature and electric field were not influencing cell detachment, the plasma torch was turned upside-down. A glass Petri dish was suspended above the torch nozzle exit on two metal rods attached to the torch support, and the plasma jet brought in contact with the bottom of the Petri dish. The power to the torch was raised until the temperature at the cell-glass interface was 49°C, measured by direct contact with the type K thermocouple mentioned above. The temperature was held constant for up to 2 minutes, and the affected area of cells examined under the microscope. As glass does not block the electric field, this was an efficient way to measure the effect of the temperature and electric field on the cells.

3.4 Transplanted cells

The cells detached and floating after plasma treatment were immediately transferred to a new Corning® 35x10 mm Petri dish. HepG2 cells were able to reattach within 5 minutes, while no HAAE-1 cells were observed to adhere. Reattachment was observed within 15 minutes. The media was changed to ensure that any oxidation of the media components did not affect the cells.

Reattached HepG2 cells were stained with propidium iodide (PI) or 3-[4,5-dimethylthiazol-2-yl]-2,5 diphenyltetrazolium bromide (MTT assay, ATCC, Manassas, VA), to ensure the viability of the cells. PI (Sigma-Aldrich, Canada) is a fluorescent dye that binds to nucleic acids (excitation at 535 nm, emission at 617 nm). PI diffuses into cells whose membrane has been disrupted, causing the cell nucleus to fluoresce. A cell whose membrane has been disrupted is generally interpreted as non-viable, however it is also possible for the cell to overcome damage to the membrane and reseal. After a given amount of time in the incubator after transplantation, reattached cells were rinsed with PBS, covered with PI solution (50 μg/mL in PBS) and left in the dark for 20 minutes. Cells were rinsed three times with PBS and visualized under the Leica DC300 fluorescent microscope (Leica Microsystems, Canada).

MTT is a yellow solution that reduces to a purple salt in the mitochondria of living cells. It is traditionally used to measure the proliferation rate of cells, however due to the small number of cells in these experiments and the uncertainty in the cell count, it was used only to ensure that reattached cells were still viable. The rate of proliferation was not measured. Briefly, 10 $^{v}/_{v}$% MTT was added to the cell culture and left in the incubator for 4 hours. One dish without cells was used as a blank. The formation of formazan was confirmed under the microscope, and 100 $^{v}/_{v}$% of detergent was added. The samples were covered and left overnight at room temperature. The absorbance of the solution was read at 570 nm in a UV/VIS spectrophotometer (Cary 100 Bio, Varian, Canada).

3.5 Functionalization

Sterilized, bacteriological-grade, polystyrene (BGPS) Petri dishes (Fisherbrand™, Fisher Scientific Canada) were exposed to the plasma jet and moved at a constant distance from the torch nozzle, forming a functionalized track on the surface. Both the 500 μm and 150 μm diameter nozzles were used. The sweep velocity ranged from 0.3 to 3 cm/s. The functionalized track width was visualized using the adhesion of HAAE-1 cells stained with crystal violet under a light microscope (Leica DC300).

Contact angles were taken to get a measure of the wettability of the surface. The contact angle is defined as the angle formed between the edge of a water droplet dispensed on a given surface and the plane of that surface. A contact angle of 180° represents a highly hydrophobic surface (ie. Teflon), while a contact angle of 0° signifies a highly hydrophilic surface. Due to the small size of the plasma jet, a crisscross pattern was drawn with the torch over a 1x1 cm^2 surface area to ensure symmetric spreading of the drop. The contact angles were measured with a goniometer (OCA 20, DataPhysics Instrument, Germany) equipped with the SCA 20 software. 2 μL droplets of distilled, deionized water at room temperature were used and analyzed with a Laplace-Young fit.

4 Results

4.1 Optimization of the O_2 gas flow rate

Before beginning work on biological substrates, the flow rate of oxygen injected through the capillary electrode was optimized to maximize the production of atomic oxygen (O) in the plasma afterglow. The reactive species are hypothesized to be the main active component in the APGD-*t* (ie. the electric field leaking out of the interelectrode region and the UV photons produced in the jet have a negligible effect). Optical emission spectroscopy was used to measure the amount of species present at the nozzle exit: it is assumed the peak in intensity of the emission line associated with the atomic oxygen species is a direct indicator of

its concentration. The strong atomic transition line of oxygen corresponding to the 3 ^{5}S – 3 ^{5}P transition (777 nm) was used. The OES measurements were taken approximately 0.5 mm downstream from the nozzle exit plane of the APGD-*t*.

The flow of helium was kept constant at its nominal value of 1 L/min, while the flow of oxygen through the capillary varied from 0 – 50 sccm. Figure 12 shows that a maximum in the peak intensity of the O (777 nm) line occurred at an O_2 flow rate of ~3 sccm, or 0.3 v/v%. The peak intensity of helium (706 nm) decreases with the addition of oxygen.

Increasing the flow of helium, while keeping the oxygen flow rate constant at 0.003 L/min, also increased the intensity of the oxygen line with a plateau occurring at 1.25 L/min (Figure 13). The higher He flow enhances the convective transport of species further downstream. On the other hand, this process is eventually counter-balanced by the additional convective cooling which leads to a decrease of the electron and gas temperatures and thus, of the density of species responsible for the O excitation.

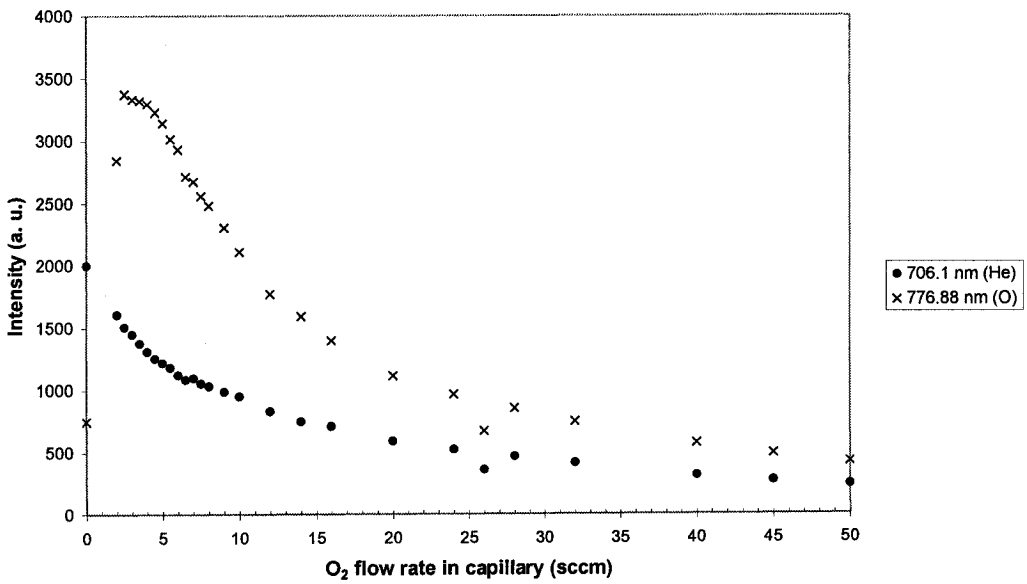

Figure 12. Relationship between oxygen added into the capillary, and the peak intensity of the O (777 nm) and He (706 nm) atomic emission lines. Helium flow rate was kept constant at 1 L/min.

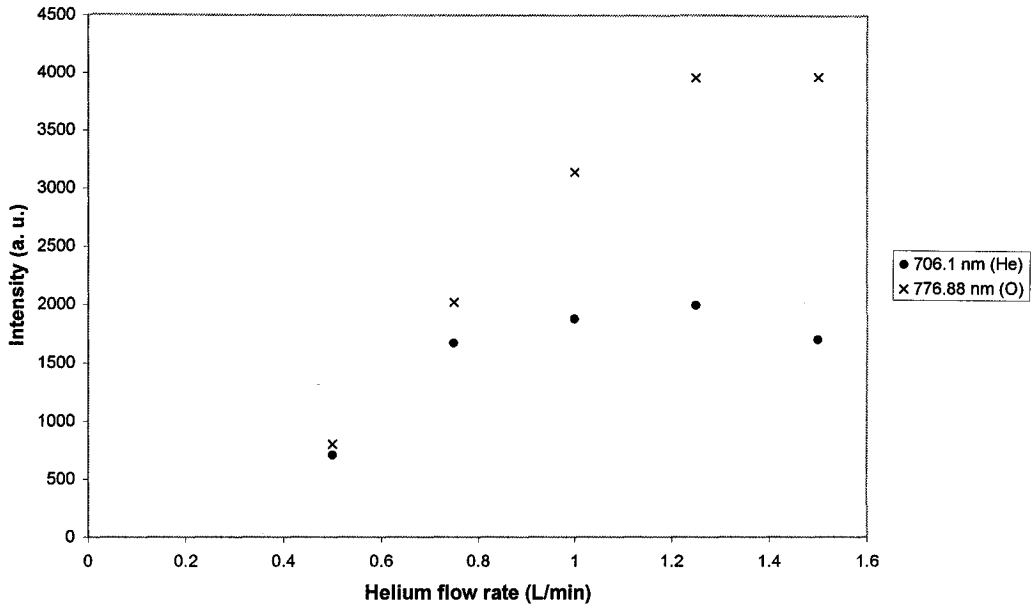

Figure 13. Effect of the helium flow rate on the peak intensity of the O (777 nm) and He (706 nm) atomic emission lines. The flow rate of oxygen was kept constant at 0.003 L/min.

The effect of modulation frequency was also investigated in order to find out whether shorter ON and OFF times would lead to a more significant production of atomic oxygen. Figure 14 shows that no change in the peak intensity of the O (777 nm) atomic emission line, as well as the He (706 nm) line, was observed over the 10 to 1000 Hz pulse modulation frequency range. In fact, additional measurements up to 100 000 Hz (not reported) showed no effect. The variability in the observations was greatest at low frequencies, when the ON/OFF cycle was visible with the naked eye, although the integration time of the OES spectrometer was still much longer than the pulse. At high frequencies, the torch does not light because the pulse time is shorter than the ramp time required to get to full power. Figure 15 shows typical square waveforms of the circuit current at 100 Hz and 100000 Hz for a duty cycle of 10%. Note that at 100000 Hz, the ramping is amplified due to the short ON period to the point where the modulation no longer appears square, and the maximum current is < 200 mA, compared to ~ 300 mA at 100 Hz under the same operating parameters.

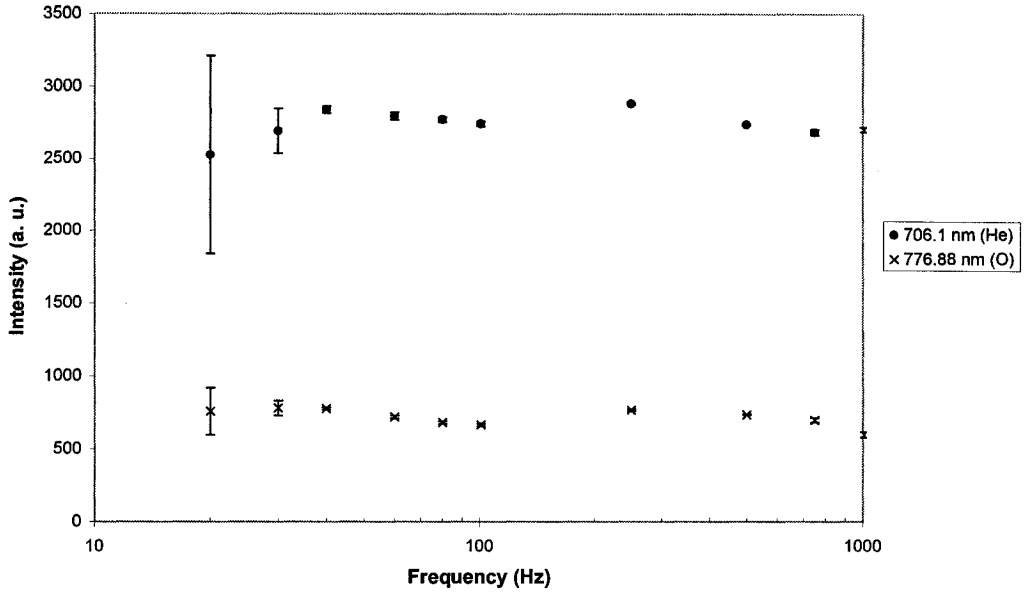

Figure 14. The effect of the modulation frequency on the peak intensity of the O (777 nm) and He (706 nm) atomic emission lines. The oxygen and helium flow rates were 0.003 L/min and 1 L/min, respectively.

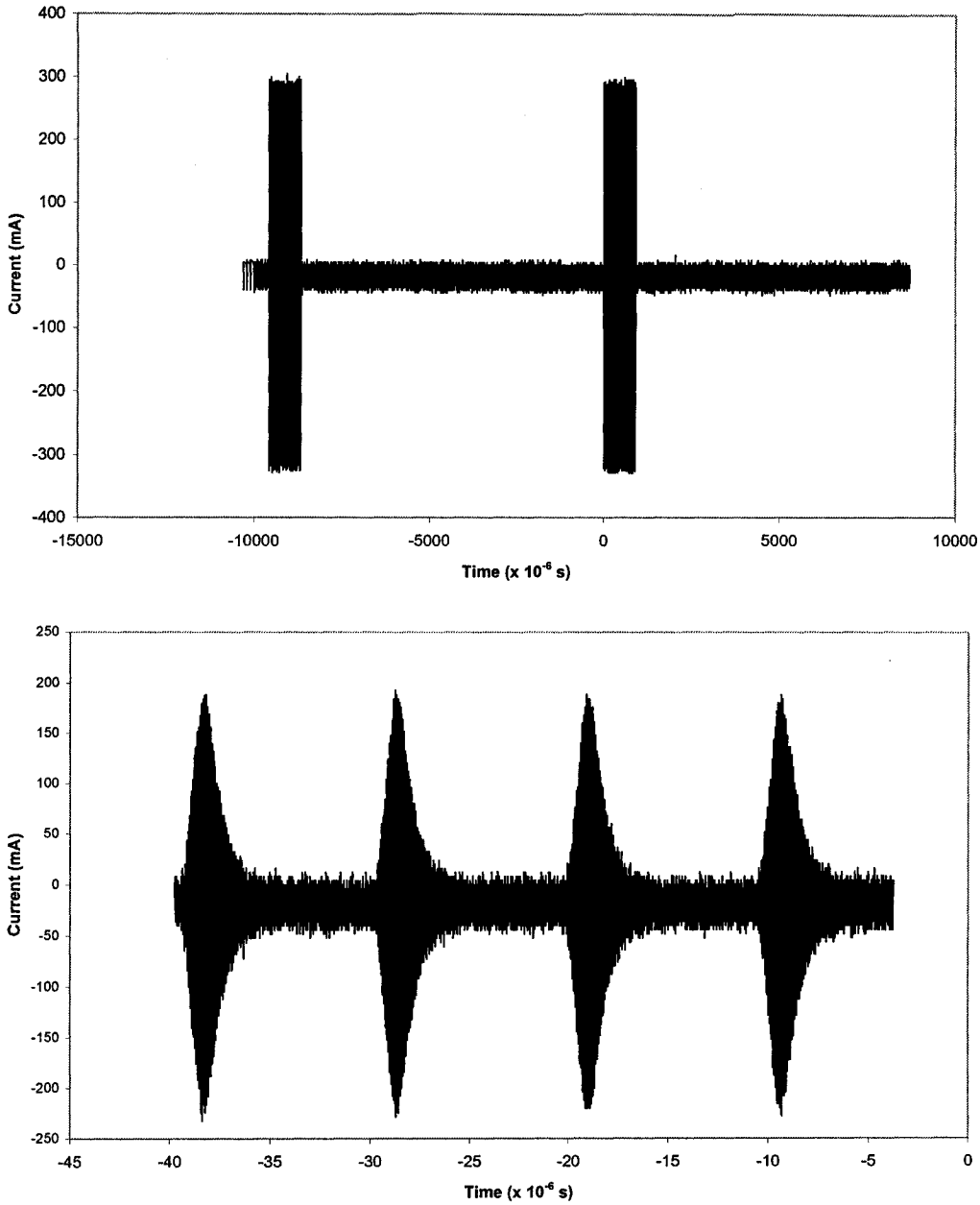

Figure 15. Typical square modulation of the RF circuit current at 100 Hz (top) and 100000 Hz (bottom) at a duty cycle of 10%.

4.2 Cell detachment from a culture vessel

The considerable gas flow through the torch nozzle (1 L/min which corresponds to a velocity of ~85 m/s and a Reynolds number of ~350 using a characteristic length of d = 0.5 mm and neglecting the effect of the capillary [6]), although essential in creating the plasma jet, could desiccate, deform or

mechanically shear the cells from the substrate. To minimize these effects on the cells, the following variables were optimized: the distance from the torch nozzle exit to the cells, the exposure time and height of media covering the cells. Optimized operating conditions were attained when the gas flow was not able to detach cells on its own, while exposure to the plasma was still able to detach cells. These parameters vary with cell line. The optimized conditions for cell removal for HAAE-1 and HepG2 cells are listed in Table 4.

Table 4. Optimized conditions for cell removal.

Parameter	HAAE-1	HepG2
Media height (mm)	1	0.5
Torch-substrate distance (mm)	2	2
Sweep velocity (cm/s)	0.33	0.33

When there was no media covering the cells, no cell detachment was observed in either cell line. Figure 16 shows cells exposed to the gas flow with no media coverage. The cells in the path of the gas stained blue with trypan blue, indicating a loss of membrane integrity, while the surrounding cells remained viable.

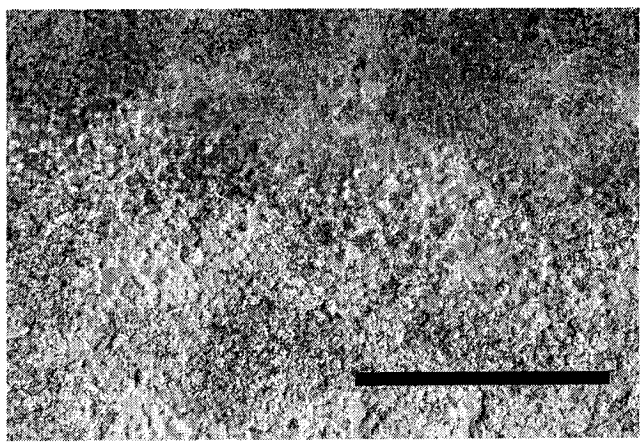

Figure 16. Cells with no media coverage exposed to gas flow incur damage to the cell membrane, indicated by the blue (dark) staining. Bar represents 250 μm.

Figure 17 shows the voids left in HepG2 and HAAE-1 cell cultures after exposure to the gas flow (top) and the plasma jet (bottom) at optimal conditions.

In both cell lines, a clear track is evident in the plasma treated dishes. The width of the void is similar, however the track was much better defined in the HAAE-1 cells.

a)

b)

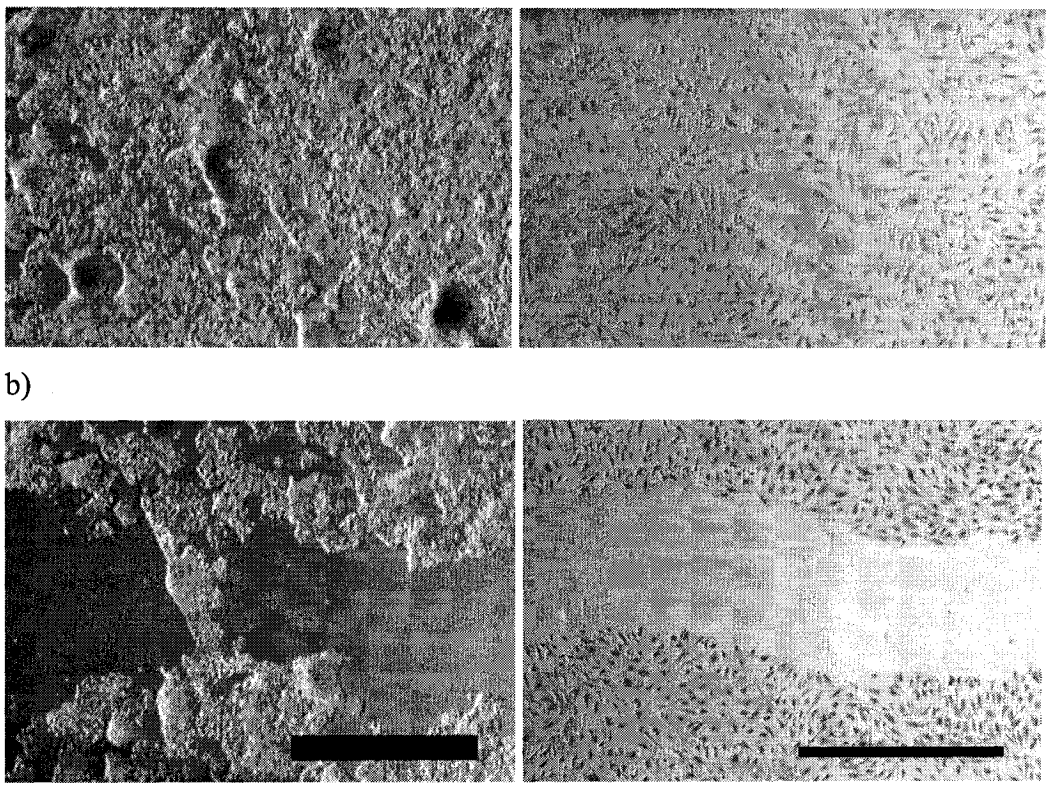

Figure 17. Cell removal of cultured HepG2 (left column) and HAAE-1 (right column) cells. Cells were exposed to the gas flow only (a) and the plasma (b) at optimized conditions. No cell detachment is observed when the cells are only exposed to the gas flow. The dark spots on the pictures on the left represent cells that are growing in a stack. Bar represents 1 mm.

The cells bordering the void during cell removal at optimal conditions initially stained blue with trypan blue (figure 18a), while after 24 hours the border was made up of cells whose membranes were intact (figure 18b).

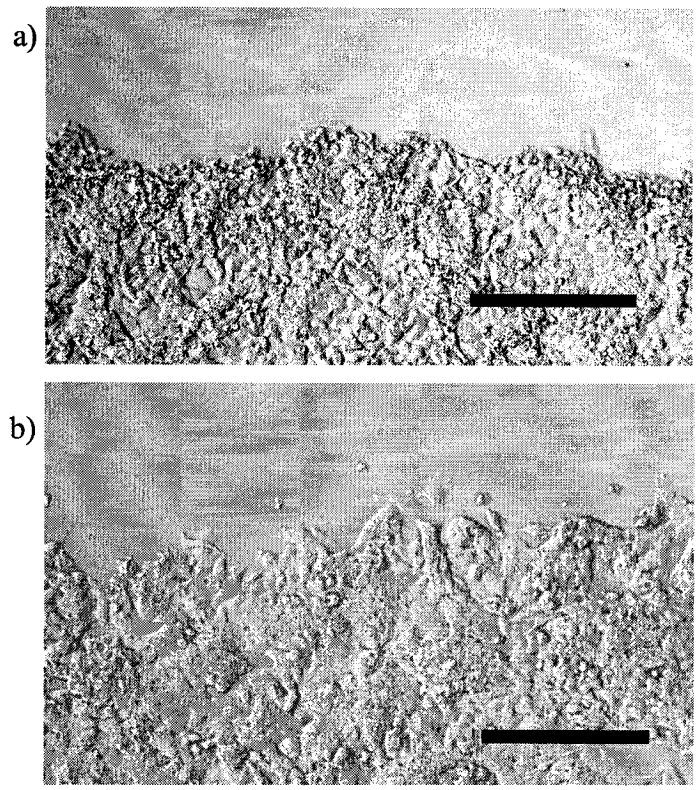

Figure 18. Border of plasma treated void in HepG2 cell culture immediately after treatment (a) and 24 hours after treatment (b). Some cells along the border initially stained blue with trypan blue, indicating damage to the membrane. Bar represents 250 μm.

To test the effect of the temperature and electric field of the plasma jet on the cells, the plasma torch was turned upside-down and directed at the bottom of a Petri dish. This protected the cells from the reactive species but did not block the electric field or thermal load. HepG2 cells exposed to a temperature of 49°C for 2 min (hotter and longer than actual treatment parameters) did not show any changes in morphology (results not shown).

4.3 Cell transplantation

The viability of the cells removed from the culture dish during plasma treatment was subsequently investigated. When cells were immediately transferred to a new culture dish, HepG2 cells were able to reattach, while HAAE-1 cells were not. The HepG2 cells that reattached were primarily found in lamellae, although there were also a few individual cells that were successfully

transplanted. The cells were observed to reattach within 5 minutes of being transplanted – cells that were still floating after 5 minutes did not reattach after 24 hours.

The reattached cells were stained with PI and observed under the fluorescent microscope. Figure 19 shows a time series of sets of cells stained with PI, with one photograph taken with the light microscope, and the second of the same area but under the fluorescence microscope.

a)

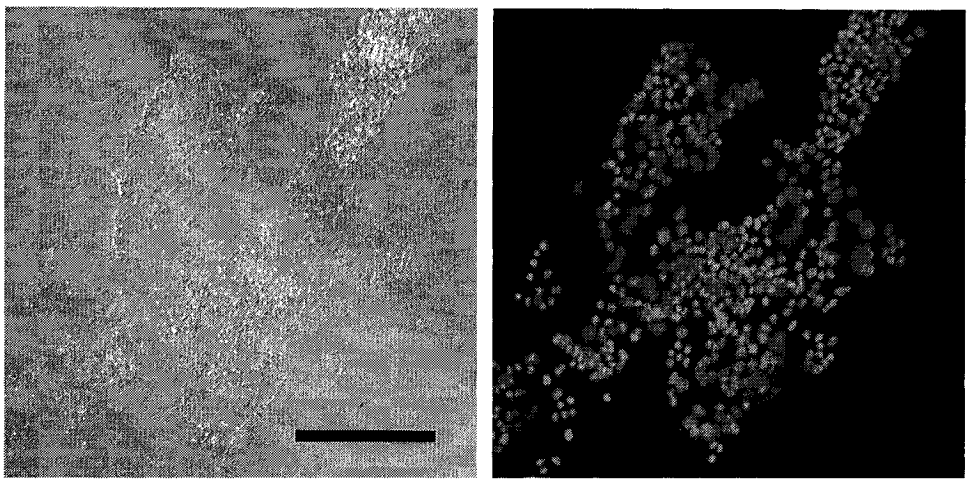

b)

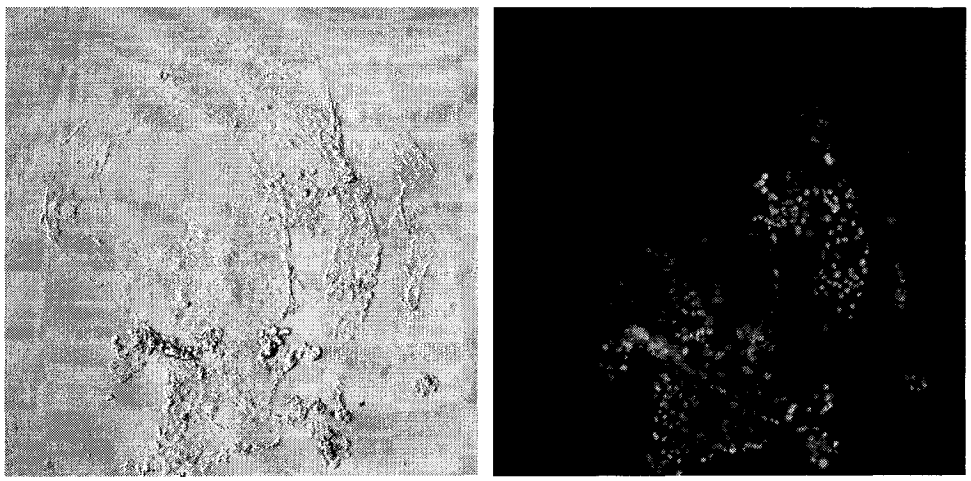

c)

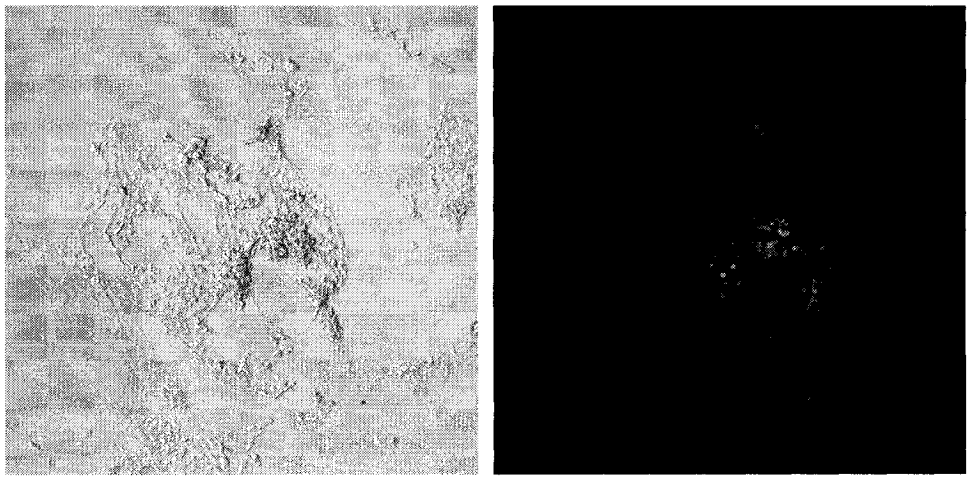

Figure 19. Time series photos showing the resealing of the HepG2 cell membrane under the light microscope (left) and fluorescent filter (right). Pictures were taken 2 h (a), 8 h (b) and 18 h (c) after plasma treatment. Cells were stained with propidium iodide immediately prior to taking the picture. The percentage of cells that fluoresce with PI decreases over time. Bar represents 250 μm.

As cell adhesion is an active process (dead cells float), and the cells remained attached to the culture dish, the transplanted cells were assumed to remain viable after plasma treatment. An MTT assay was used to support this hypothesis. Instead of a diffusion process like the transport of PI across the cell membrane, MTT is a chemical that is reduced in the mitochondria to create a purple salt (formazan crystals). A viable, proliferating cell is required to metabolize the compound and to produce the purple precipitate. Figure 20 shows the formazan crystals formed in the reattached cells. After the solubilization of the crystal, the re-adhered cell sample had a significantly higher absorbance reading than the blank, indicating that the reattached cells were indeed viable and proliferating up to 7 days after treatment. The actual absorbance values have not been included as they vary with cell count, making the absolute values incomparable. Due to the low sample size, it was very difficult to obtain an accurate cell count, and therefore to get a comparable measure of the proliferation rate.

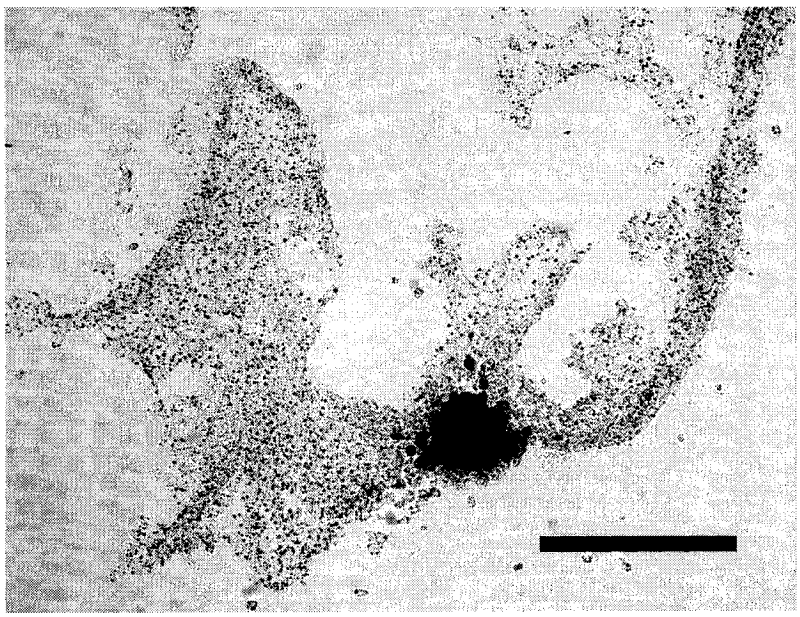

Figure 20. Reattached HepG2 cells stained with MTT. Little purple dots are the formazan crystals, indicating a functioning mitochondria. Big purple clump corresponds to cells growing on top of each other. Bar represents 250 μm.

4.4 Surface functionalization

The contact angle of distilled, deionized water on BGPS, BGPS functionalized with helium, and BGPS functionalized with He + 0.3% O_2 in the capillary of the APGD-*t* is presented in Table 5. The results clearly show that the plasma treatment significantly ($P<0.05$, ANOVA) decreased the contact angle on the treated surfaces.

Table 5. Contact angle of distilled, deionized water on pristine and treated polystyrene (n=6).

Surface	Contact Angle (°)	Standard Deviation (°)
Untreated BGPS	92.7	3.0
BGPS – He plasma treated	35.0	0.5
BGPS – He + 0.3v/v% O_2 plasma treated	35.7	1.0

Figure 21 shows the preferential cell attachment on the plasma treated area. Adhered cells were stained to visually identify the width of the functionalized track. Both the 500 μm and 150 μm torch nozzles were used to attempt to vary the width of the track.

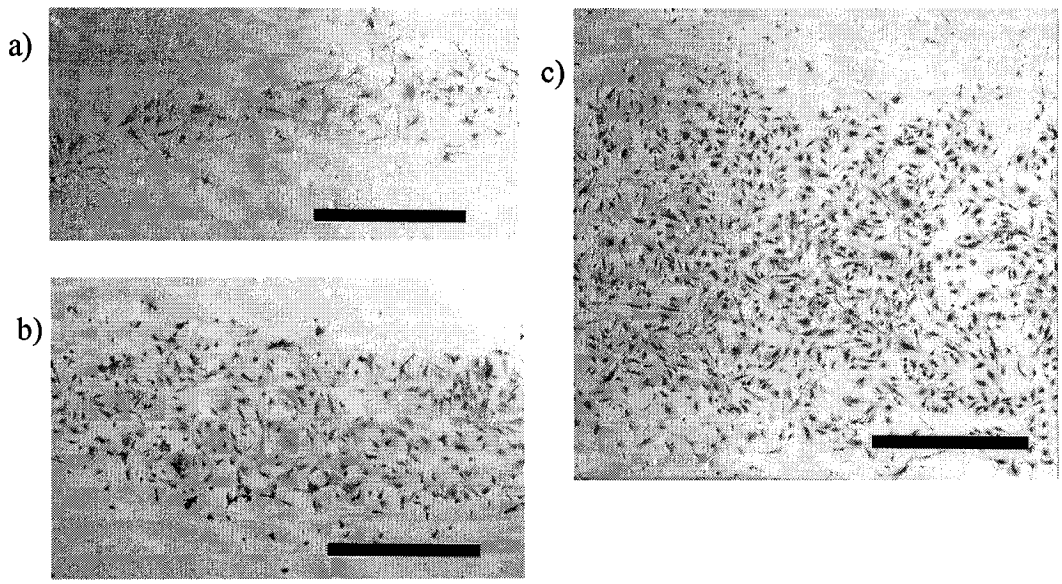

Figure 21. Cells adhered on functionalized tracks created on BGPS Petri dishes by the APGD-*t* 24 h after seeding. The width of the track can be controlled by the size of the nozzle and the sweep speed. A sweep speed of ~ 3 cm/s and a torch-substrate distance of 1 mm were used for tracks a) (150 μm nozzle) and b) (500 μm nozzle). A slow sweep speed (~ 0.5 cm/s) vastly increases the track width (c). Bar represents 1 mm.

Figure 22 shows the effects of the torch-nozzle distance and the sweep speed on the track width, while Figure 23 shows the preferential spreading of water along the functionalized tracks at various torch-nozzle distances.

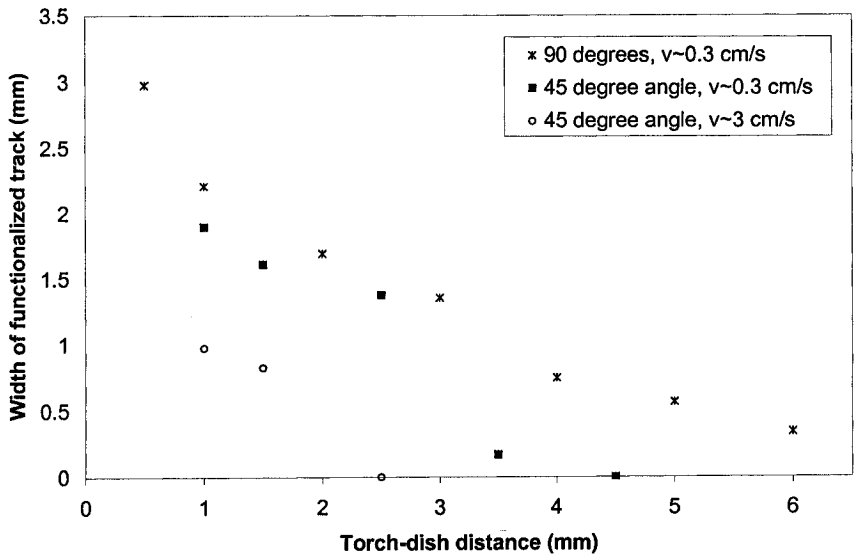

Figure 22. The width of the functionalized track, visualized with the adhesion of HAAE-1 cells on the surface, as a function of the distance between the torch nozzle exit and the substrate. The angle between the torch and the substrate was varied, as well as the sweep speed using the 500 μm diameter nozzle. * – 90° (APGD-*t* is perpendicular to the surface), *v* ~ 0.3 cm/s; ■ – 45°, *v* ~ 0.3 cm/s; ○ – 45°, *v* ~ 3 cm/s (n=1).

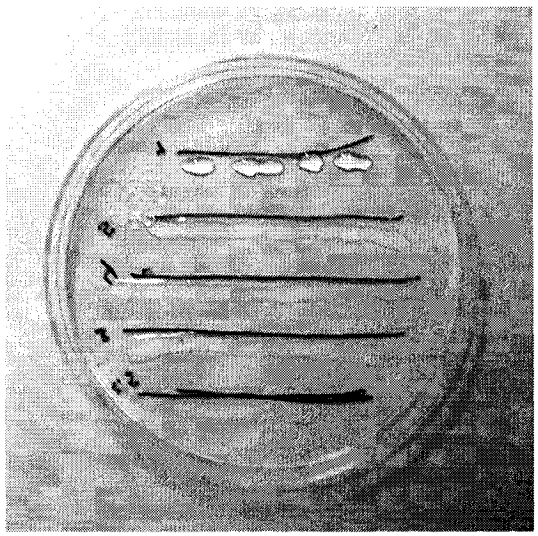

Figure 23. Functionalized tracks along a BGPS dish. Tracks were functionalized below the black line at a torch-substrate distance of (starting from bottom of dish) 2.5, 3, 4, 5 and 7 mm. Up to d = 5 mm, the water naturally spreads along the track, whereas at 7 < d < 10 mm, the water will rest preferentially on the functionalized area after having been mechanically moved with the pipette tip.

5 Discussion

The results of the first set of experiments demonstrate the effects of the APGD-*t* on cultured mammalian cells. The gas flow was optimized to maximize the production of ROS, which is expected to be the primary element involved in any cell treatment or surface funtionalization experiments. The torch was able to detach cultured cells and in the HepG2 cell line, the cells were temporarily permeabilized and remained viable up to 7 days after treatment.

In a second set of experiments, the torch was used to functionalize BGPS surfaces to improve cell adhesion. The experimental parameters were optimized in order to attain the smallest track width possible to improve its potential as a biological micropatterning tool.

5.1 Torch Optimization

The experiments demonstrate that the APGD-*t* can locally detach cells, and radicals such as OH, O and N_2 produced by the plasma are believed to be the cause of this cell detachment [6]. Initial experiments, however, showed that when

using the plasma torch for cell treatment, an elevated gas flow could desiccate or mechanically shear the cells from the culture surface. Therefore, the desire to maximize the production of reactive species was countered with the need to protect the cells from the shear. A helium flow rate of 1 L/min as the plasma-forming gas provided a good balance between these two variables.

The oxygen injected into the capillary was set at 3 sccm, which corresponded to a maximum peak intensity of the O (777 nm) line. This maximum oxygen intensity at such a low flow rate could be due to competing reaction mechanisms within the plasma jet. After reaching a maximum peak intensity, the electrons could be used in the excitation, and not dissociation, of oxygen, or in competing reactions with other species, leading to a decrease in the 777 nm line. There was no observed increase in peak intensities coupled with the decrease in the O (777 nm) line to elucidate possible competing reaction pathways. The continual decrease in the helium (706 nm) peak intensity with the addition of oxygen is also likely to be caused by the competing reactions, leaving fewer electrons available to excite the helium.

Given the flow rate of the plasma-forming gas, the modulation frequency was investigated in order to maximize the production of reactive species. It was hypothesized that a higher modulation frequency could result in an increased radical production. By pulsing more often for a shorter interval of time (keeping the duty cycle constant), it was thought that the recombined species could be immediately re-excited (decreasing the lag time until the next pulse), thereby increasing the concentration of reactive species. In fact, such a hypothesis was invalidated. There was no observed increase in the atomic oxygen line (777 nm) or helium line (706 nm) over modulation frequencies of 10 to 100000 Hz.

Based on those observations, it was decided to keep the amplitude modulation frequency at 100 Hz, which is high enough to reduce to OES variability without introducing a high-pitched noise that is coupled with operation at higher frequencies.

5.2 Effect on cells

The effect of the APGD-*t* operating under optimized conditions was tested on cultured cells. The distance from the torch to the cells was selected to ensure that cells did not detach due to the mechanical shear imposed on the cell, but still allowed the transport of plasma species to the culture. The width of the void left in HAAE-1 cultures after exposure to the plasma jet is approximately 750 μm, or 1.5 times the inner diameter of the nozzle (Figure 17). The void left in HepG2 cultures varied in size and shape, likely due to strong cell-cell adhesion resulting in the detachment of lamellae, rather than individual cells.

The estimated shear created by the gas flow alone is less than the reported force needed to detach similar cell lines [70] (see Appendix 2 for more information and discussion). The electric field and thermal load alone were not able to detach cells. To ensure that the combined effects of the electric field and thermal load with the gas flow do not shear the cells, it would be beneficial to repeat this experiment while simultaneously exposing the cells to the gas flow. This would require a second torch above the Petri dish, connected to the gas lines.

If the electric field were to reach the cell, this could affect the cell in a few ways depending on the field strength. At low electric fields, a dipole is induced in the cell which can be used to move and manipulate a cell, while at field strengths of 1 kV/cm, the cell membrane can be permeabilized [71]. Fields of 100 kV/cm can damage ion channels and denature proteins due to the increase in supramembrane potential; the effect of Joule heating is negligible [72]. The electric field at the powered capillary electrode is calculated to be ~ 10 kV/cm at 810 V_{ppk}. Theoretically though, the electric field should only occur between the two electrodes, and should not pass to the cells unless a transfer of current (bright filament formed between torch and substrate) is observed. The electric field also decreases with distance from the powered electrode to ~1 kV/cm at the ground electrode, and would be even lower at the cell interface as the torch-substrate distance is twice the electrode gap

When optimizing the variables listed in Table 4 to reduce the impact of the gas flow on the cells, the height of the media had the most substantial effect on

cell detachment. The media most likely provided a cushioning effect for the cells - the jet had enough momentum to displace the media, leaving a liquid layer thin enough for the reactive species to penetrate through to the cells, without sufficient mechanical shear to remove the cells from the substrate. The variation in the media height required for optimized plasma treatment is likely due to the different growth conformations of the cells and adhesion forces. HAAE-1 cells grow in a monolayer as distinct cells, whereas HepG2 cells tend to grow very tightly packed and will even stack.

In experiments with no media coverage (Figure 16), the gas flow could have flattened the cells and damaged the cell membrane, allowing trypan blue to diffuse into the cells. The media coverage in optimized conditions is likely to protect the cells from the full force of the gas impinging on the cells. During clinical use, a saline gel could be used to cover and protect the tissue during plasma treatment.

For media heights of $0 < h <$ optimal, the gas was able to detach cells. The movement of the media created by the gas flow could have created enough shear to detach the cells from the surface, as the viscosity of water is much higher than air. At $h \geq$ optimal the shear could have dropped below a critical value required to detach cells. However if the media height is too large, the species will not be able to reach and react with the cells. Further study into the fluid dynamics of the system is required to fully understand the effect of the media coverage.

As the gas flow had such a pronounced effect on cell detachment, a blank run with gas flow only was done before each experiment. Taking a look once more at Figure 17, a comparison of the cell detachment due to the gas flow only and the plasma can be made (operating at optimal conditions). Although the gas is capable of detaching some cells at optimized conditions, there is a significant increase in cell detachment once power is applied to the torch. As the heat, electric field and gas flow were not able to detach cells on their own accord, it is expected that the reactive species in the plasma jet are responsible for the cell removal.

The cells remaining on the Petri dish after plasma treatment were viable. In some areas, a row or two of cells right on the border of the void in HepG2 cultures stained blue with trypan blue (Figure 18a). Some of the blue cells were attached to the Petri dish, while others were floating about, only anchored to other viable, adhered cells. The rest of the cell culture looked unaffected by the plasma treatment. After 24 hours, cells along the border no longer stained blue, meaning that they either detached and were floating in the media, or had been permeabilized and were able to reseal their membranes (Figure 18b).

5.2.1 Possible reactions resulting in cell detachment

Cell detachment due to the reactive species in the plasma jet could be due to the oxidation (and cleavage) of the adhesion proteins found on the exterior of the cell. Generally speaking, proteins can undergo extensive oxidation with only minimal effects on their function. Singlet oxygen, the hydroxyl radical, hydrogen peroxide and $ONOO^-$ can readily oxidize the amino acid building blocks of the proteins [34]. By fragmenting the adhesion proteins, the anchoring junctions can be cut, detaching the cell from the substrate and other cells.

An interesting effect that must be accounted for is that most HepG2 cells floating in the media after plasma treatment were in lamella. The breaking of the cell-matrix bond while keeping the cell-cell junctions intact could indicate one of a few things. The first is that the integrins are more easily oxidizable than the cadherins. Integrins have a specific proteolytic cleavage site (the –S-S- bond on the α unit) and have been designed for an easy breakdown. Amino acids groups like the histidine-alanine-valine sequence found in the extracellular domain of the cadherin protein can be oxidized by RNS and ROS, however there is no specific proteolytic cleavage site [34, 73].

Another possibility is that the configuration of the cell-cell anchoring junctions creates a stronger bond than the cell-matrix junctions. Patches of adhesion proteins hold the cells to the matrix, while cell-cell adhesion is further supported by the continuous ring of adhesion between cells given by adherens junctions.

In terms of individual bond strength, the force required to disrupt single cadherin-cadherin and integrin-ligand bonds are both in the order of pN [74, 75]. Experiments have also been done to quantify the adhesion force between cells and the matrix. The shear force required to push off a murine fibroblast cell with a miniature cantilever from polystyrene treated for tissue culture was ~300 nN after an incubation period of 24 h [70, 76]. The adhesion force was dependent upon the substrate used, and ranged from 260 - 882 nN. The force required to pull apart two S180 cells in suspension transfected with E- and N- cadherin was about 200 nN after 1 h of contact time, at which point the authors report the force reaches a plateau [77].

The adhesion strength for the cell-cell and cell-matrix bonds in these studies are on the same order, leading one to believe that cell-cell bonding is no stronger than cell-matrix bonding. A longer incubation time could, however, increase the individual cell-cell adhesion strength. Cells growing in a confluent culture could form a stronger cell-cell matrix, as the adhesion belts would be used to their full potential.

From a fluid mechanics standpoint, the geometry of cell growth makes the cell-matrix bond more susceptible to shear. The cell-matrix interface will be influence by the shear, whereas the cell-cell bonds will be affected by pressure at the stagnation point. The shear could be partially responsible for the cells lifting off in lamellae, once the adhesion proteins had been oxidized.

A third theory concerning the cells detaching in sheets is that the reactive species are targeting the integrin's ligand receptor, leaving the adhesion proteins unaffected. Collagen, laminin and fibronectin are all found in the basement membrane, and are receptor ligands for, amongst others, the $\alpha 2\beta 1$, $\alpha 6\beta 4$ and the $\alpha 5\beta 1$ integrins, respectively. Hydroxyl radicals and ozone have been shown to be able to degrade soluble type I collagen, and at low concentrations cause the collagen to become more susceptible to proteolytic degradation [78]. To target the ligands in the basement membrane, the reactive species would have to diffuse through the media and the cells without reacting. Therefore, species with high reactivities and low lifetimes such as the hydroxyl radical would not be involved

in any reactions with the ligands. There is debate over whether singlet oxygen, considered to have a relatively long lifetime, will be able to diffuse through the cell membrane, never mind all the way through the cell [17]. While the oxidation of the ligands would provide a nice explanation regarding the detachment of cells in lamella, the species responsible for the oxidation reactions would have to be long lived and have a high enough reduction potential to initiate the reaction. The permeabilization of the cell membrane also indicates that there is oxidation occurring at the exterior of the cell, and that the adhesion proteins should be targeted along with the membrane lipids.

Cell detachment is an active process, and could also result from the apoptosis of the cell due to an imbalance of oxygen or nitrogen within the cell, however the time scale for this reaction would be much longer than the oxidation reactions. More work is needed to elucidate the exact cause of cell detachment.

5.3 Cell transplantation

There was some evidence to support the hypothesis that the removed cells would remain viable after plasma treatment. HepG2 cells were able to reattach in a new culture vessel, whereas HAAE-1 cells did not. This difference could be attributed to different tolerances to ROS, and therefore the parameters used could have been too intense for the HAAE-1 cells and could have ruptured their membranes, while only permeabilizing the membrane of the HepG2 cell.

From Figure 19, it is evident that the percentage of reattached cells that fluoresce with PI decreases with time. All of the cells fluoresce up to 4 hours after plasma treatment, while very few fluoresce after 24 hours. This indicates that initially there was damage to the membrane that allowed PI to penetrate into the cell and react with the nucleic acids (Figure 19a), however the cell was able overcome the trauma and repair its membrane, blocking the PI from entering the cell (Figure 19c). The MTT assay revealed that all reattached cells displayed purple staining and were therefore metabolically active for up to 7 days after treatment, although little proliferation of the cells was observed during this time.

It is hypothesized that the HepG2 cells underwent non-fatal lipid peroxidation resulting in the temporary permeabilization of the cell membrane, as opposed to a complete rupture of the membrane. This would account for PI diffusing into the cell, as well as the continued cell adhesion. Cells permeabilized by other techniques have been shown to be capable of resealing and remaining viable, while others remain active for a short period of time before apoptosis [79]. The electric field is likely not the primary cause of permeabilization, as it takes between 4 – 24 h for the cells to reseal, whereas the resealing time is ~ 1 s after electroporation [53]. The longer time scale needed by the cell to recuperate after plasma treatment suggests more than just a rearrangement of the cell membrane, but rather potentially a partial chemical degradation of the membrane initiated by the reactive species from the plasma jet.

Certain reactive oxygen species (OH•, HO_2•, RO•, RO_2•) and ozone have enough energy to cleave a hydrogen from the double bond on the PUFA, initiating lipid peroxidation [34, 80]. This begins a chain reaction which can result in the crosslinking of lipids, or the formation of peroxide molecules through the reaction with oxygen. The peroxides can be further decomposed to aldehydes, ketones and hydrocarbons. Singlet oxygen, while not able to initiate the reaction, can increase its propagation rate. The crosslinking of the lipids decreases the fluidity of the membrane, and the fragmentation of the molecules increases the permeability of the membrane. This can allow passage of species into the cell that would not normally be able to diffuse across the membrane. Eventually, the lipids may break down to a point where the membrane loses its structural integrity, and the cytosol leaks out of the cell. In this case, the damage is irreversible and the cell is no longer viable.

In the present case, propidium iodide has a molecular mass of 668 Da, indicating that the pores formed in the cell membrane must be at least this size. Therefore, it is possible to insert relatively small markers into the cell without necrosis. Proteins and DNA are on the order of kDa-MDa (diameter of plasmid DNA ~ 10 nm [57]), so it is uncertain if the pores created by the APGD-*t* are big

enough for gene therapy or electrochemotherapy. The pore size is likely dependent on the treatment parameters, namely torch power and exposure time.

5.4 Functionalization of polystyrene Petri dishes

When functionalized with the plasma torch, the contact angle on the BGPS Petri dish decreased from 93° to 35° (Table 5). The addition of oxygen in the capillary did not affect the contact angle, likely because at the treatment plane, the entrainment of air in the plasma jet saturates the jet with oxygen and nitrogen species. Other studies into the surface modification of polymers by a plasma have related the change in wettability to an increase in the percentage of nitrogen and oxygen groups (C-N, C-O, C=O, O-C=O) present on the surface [68, 81].

The functionalized polystyrene Petri dishes were sent for preliminary XPS analysis. The early results found traces of silicon on the surface, most likely a mould release agent used in the manufacturing process, and scratches on the surface. To overcome this, a thin film of polystyrene was deposited on silicon wafers, ensuring a flat surface and a pure polystyrene base. It has not yet been possible to analyze the new samples. It is expected that there will be an increase in oxygen and nitrogen groups found on the surface, in accordance with other studies. Other reactive species such as excited O, N_2 and N_2^+, and OH radicals are suspected to participate in the functionalization of the surface and have been observed in the plasma jet at the axial position corresponding to the interface with the polystyrene substrate [32].

Cell cultures can be used as a visual confirmation of surface functionalization (Figure 21). An increase in hydrophilicity due to the addition of polar functional groups at the surface (ie. –COOH, $-NH_2$) results in enhanced cell adhesion on a polymeric substrate [63, 82]. The cells exhibited confluent growth on the areas exposed to the plasma, while minimal growth was observed on the untreated areas. The width of the functionalized tracks is approximately twice the I.D. of the nozzle, ~350 μm for the I.D. of 150 μm (Figure 21a), and ~1 mm for the I.D. of 500 μm (Figure 21b).

The track width depended primarily on sweep speed and torch-substrate distance. To achieve the tracks shown, a relatively fast sweep velocity, ~3 cm/s, was used with the nozzle exit located 0.5 - 1 mm away from the surface. At lower sweep velocities, convection pushed the reactive species further out radially, and consequently, the width of the track increased (Figure 21c).

The effect of the torch-nozzle distance and the sweep speed on the track width can be seen in Figure 22. The width of the track decreased as the gap between the torch and the substrate increased, as more reactive species would recombine before coming in contact with the dish. A faster sweep speed decreased the track width by reducing the radial diffusion of species. Changing the inclination of the torch from 90° (normal to the surface) to 45° reduced the outwards convection of the jet, and resulted in a slight decrease in the track width. There was a critical torch-substrate gap above which the cell culture was not confluent and the track lost its crisp definition. This distance was 4 mm for a sweep speed of 0.3 cm/s.

When water was dropped onto the tracks, it spread along the functionalized tracks at torch-substrate distances of up to 5 mm, and would rest preferentially along the track after being mechanically moved at functionalization distances up to 10 mm (Figure 23). It is interesting to note that this nozzle-substrate gap is much larger than the length of the visible plasma jet (<2 mm). Reactive species like metastable helium atoms, not detectable directly through OES, could be present far downstream from the visible jet, and could cause the increase in hydrophilicity.

6 Conclusions

This body of work investigated various potential biological applications of the APGD-*t*. Before beginning work with cell cultures and substrates, the O_2 gas flow rate was optimized to get a maximum amount of reactive oxygen species at the nozzle exit. OES results showed that a concentration of 0.3v/v% oxygen added to the capillary resulted in a maximum intensity of the atomic oxygen, O (777 nm), emission line. Increasing the He gas flow rate also increased the

concentration of reactive species very close to the nozzle exit, however a flow rate of 1 L/min was used to minimize the shear on the cells.

Experiments using the plasma torch on cells support the hypothesis that it can locally detach both HepG2 and HAAE-1 cultured cells. The cause of cell removal is hypothesized to be oxidation reactions between the reactive species in the plasma jet and either the adhesion proteins or the receptor ligands. The heat, electric field and jet momentum coupled with the jet were shown not to be capable of causing cell detachment on their own. The media height, torch-cell distance and sweep speed had to be optimized to minimize the cell removal caused by the shear associated with the high gas flow. The height of the media had to be large enough to minimize the shear, but thin enough to allow the reactive species to reach the cell. As the APGD-*t* can remove cells from a culture dish, it holds great promise as a biomedical tool for localized cell removal without the pain associated with high thermal loads. If species responsible for cell removal were created in the media (ie. hydroxyl radicals from the dissociation of water), a thin film of saline gel could be applied to the skin to simulate this, much like what is used in Coblation®.

For applications in skin resurfacing, high temperatures are often used as collagen can be denatured by heat, causing the fibres to shrink [17]. Temperatures in excess of 63°C have been reported to drastically increase the rate of reaction. Although we have the ability to operate at a low temperature, the controlled application of heat in conjunction with the reaction species is always possible to enhance the treatment. Léveillé and Coulombe demonstrated that the jet temperature can be increased to 120°C if the APGD-*t* power is raised to 5 W [6].

Some evidence was provided to support the hypothesis that plasma treated cells remain viable. HepG2 cells that were detached by plasma treatment were successfully transplanted to a new culture vessel. Here, they were metabolically active for 7 days, and were able to overcome the permeabilization of the membrane within 24 hours. The cells remained permeabilized for 4 hours, after

which time they started to reseal. It is suspected that the hydroxyl radical initiated lipid peroxidation, resulting in the temporary permeabilization of the membrane.

The transient pore size is at least 414 Da, the size of the fluorescent dye diffusing into the cell. To be useful for the insertion of proteins or DNA, the pores need to be at least in the kDa range. Plasma permeabilization is able to overcome certain problems associated with present techniques, including cell death through fixing and the small sample size associated with microinjection.

In separate experiments, functionalizing BGPS Petri dishes with the APGD-*t* caused the contact angle to drop from 93° to 35°. The functionalized track was visualized using the adhesion of HAAE-1 cells. Two different I. D. nozzles were used (150 μm and 500 μm) to create the tracks, and the sweep speed and the torch-substrate distance were found to affect the track width. The skinniest tracks that were observed were approximately double the I. D. of the nozzle exit. This shows promise for micropatterning, as it eliminates the need for a mask and the chemical processing involved in photolithography. The torch could be attached to a robotic arm, and could be programmed to functionalize patterns on all surface geometries. To get tracks small enough to align a single row of cells for the study of neurons (width < 20 μm), a masking process would still need to be used. Used alone, the APGD-*t* is more suited towards larger scale patterning, for example recreating in-vivo cell patterning on an implant.

7 Future work

There is much work to be done before the APGD-*t*'s potential as a medical and laboratory tool can be realized. Studies looking into the long-term health of cells surrounding the plasma treated area need to be done to be sure that the ROS and RNS in the plasma do not have a detrimental effect on the remaining cells. *In-vivo*, the oxidation of a cell's identification proteins can alter their structure, causing the cell to look like a foreign invader and be attacked by the immune system.

For laboratory applications, quantification of the data is required to give end-users an idea of the effectiveness of the technology. For example, what percentage of the cells removed are able to re-adhere on a new dish? How does this vary with cell line? How big are the pores formed in the cell membrane? What percentage of cells is able to fully recover from plasma permeabilization? These and many more are all noteworthy, although potentially difficult, questions to answer.

It is also important to elucidate the interaction mechanisms occurring between the plasma and the cell. In particular, it would be very interesting to test for lipid peroxidation and the oxidation of adhesion proteins. These methods can be used to test for the end result of plasma treatment (lipid peroxidation or protein oxidation), but will not shed light onto the specific species involved in the reactions. Some insight into the methodology that can be used to test for these two phenomena is outlined below.

Lipid Peroxidation

A common method to measure lipid peroxidation is to measure the malondialdehyde (MDA) content of the sample with a thiobarbituric acid (TBA) test. The TBA reacts with MDA to form a pink complex, whose absorbance can be read at 532 nm, and is expressed as TBA reacting substances (TBARS). Although widely used, there is controversy over the interpretations of the results of this test. The sample preparation requires an acid heating step, which can decompose intact lipids and give readings 100x larger than those obtained with specific assays [83]. There are also other chromophores that absorb at this wavelength, further skewing the data. Modifications have been made to reduce these complications, and are outlined in Templar *et al.* [84]. Briefly, butylated hydroxytoluene is added to the sample to prevent further lipid oxidation during sample preparation, and the sample is run through the HPLC to separate the chromophores. These two steps increase the certainty that any increase in absorbance is due to the $(TBA)_2$-MDA complex.

Another way to determine if lipid peroxidation is occurring is through the use of a stain. These chemicals will react with products of lipid peroxidation, and the change in fluorescence can be visualized under a microscope. Unfortunately, many of these stains will fluoresce upon contact with smaller ROS such as the hydroxyl radicals or hydrogen peroxide. These could be generated by the plasma and come into contact with the stained cell, giving a false positive reading. Diphenyl-1-pyrenylphosphine (DPPP) is a fluorescent stain that will only react with hydroperoxides, and not H_2O_2 or OH• [85, 86]. This specificity comes with a price however – to read the blue fluorescence the cells need to be excited at 351 nm, and the emission read at 380 nm, two non-standard wavelengths in fluorescent microscopy. This requires the use of a microscope with variable wavelength filters, or custom made filters, which are a significant additional cost.

Oxidation of adhesion proteins

Antibodies can be used to stain for the degradation of adhesion proteins. The antibodies are tagged with a fluorescent marker and will bind to specific adhesion proteins or its subunits (ie. α6 or β4 integrin subunit). Any loss of fluorescence will indicate that the selected adhesion protein is no longer being expressed. In terms of plasma treatment, it is likely to indicate that the protein has been oxidized. When staining, it is important to select an adhesion protein that is known (or highly suspected) to be expressed by the cell in question. It is also difficult to draw broad conclusions regarding cell adhesion processes through antibody staining, as the expression of one particular CAM shows only one part of the picture.

Finally, animal trials are an important step prior to clinical trials on humans. They provide a good model for potential treatment results and side effects in humans. Mouse or porcine skin can be used to measure the penetration depth of the APGD-*t*, while live animals would need to be used to study wound healing.

These are just a few of the potential areas that can be explored in the future regarding the interaction of the APGD-*t* with mammalian cells and tissue.

Before beginning work, it would be worthwhile to examine Appendix 3, which details some of the less successful experimental approaches taken during this work. This will hopefully save future researchers time, and direct them along the right path. As plasma in the medical field is an emerging sphere of research, there exist many possibilities for future exploration and applications.

8 References

1. Okpara-Hofmann, J., M. Knoll, M. Dürr, B. Schmitt, and M. Borneff-Lipp, "Comparison of low-temperature hydrogen peroxide gas plasma sterilization for endoscopes using various Sterrad™ models." *Journal of Hospital Infection*, **59** (2005): 280-285.
2. Stoffels, E., I.E. Kieft, and R.E.J. Sladek, "Superficial treatment of mammalian cells using plasma needle." *Journal of Physics D: Applied Physics*, *Journal of Physics D: Applied Physics*, **36** (2003): 2908.
3. Kieft, I.E., D. Darios, A.J.M. Roks, and E. Stoffels, "Plasma treatment of mammalian vascular cells: a quantitative description." *IEEE Transactions on Plasma Science*, **33** (2005): 771.
4. Fridman, G., M. Peddinghaus, A. Fridman, M. Balasubramanian, A. Gutsol, and G. Freidman. "Use of non-thermal atmospheric pressure plasma discharge for coagulation and sterilization of surface wounds." in *Proc. 17th Int. Symp. on Plasma Chemistry, Toronto, 2005*. 1066-1067.
5. Coulombe, S., V. Léveillé, S. Yonson, and R.L. Leask, "A miniature atmospheric pressure glow discharge torch (APGD-*t*) for local biomedical applications." *Pure & Applied Chemistry*, (2005): in press.
6. Léveillé, V. and S. Coulombe, "Design and preliminary characterization of a miniature pulsed RF APGD torch with downstream injection of the source of reactive species." *Plasma Sources Science and Technology*, **14** (2005): 467-476.
7. Ohl, A. and K. Schröder, "Plasma-induced chemical micropatterning for cell culture applications: a brief review." *Surface & Coatings Technology*, **116-119** (1999): 820-830.
8. Goodwin, A., *Plasma Solutions: Flexible Displays & Electronics Workshop*, http://www.linkisd.org.uk/PDF/14.plasma_solutions.pdf, as of March 2004.
9. Laroussi, M., D.A. Mendis, and M. Rosenberg, "Plasma interaction with microbes." *New Journal of Physics*, **5** (2003).
10. Montie, T.C., K. Kelly-Wintenberg, and J.R. Roth, "Overview of research using the one atmosphere uniform glow discharge plasma (OAUGDP) for sterilization of surfaces and materials." *IEEE Transactions on Plasma Science*, **28** (2000): 41.
11. Schutze, A., J.Y. Jeong, S.E. Babayan, J. Park, G.S. Selwyn, and R.F. Hicks, "The atmospheric-pressure plasma jet: A review and comparison to other plasma sources." *IEEE Transactions on Plasma Science*, **26** (1998): 1685.
12. Brand, C.U., A. Blum, A. Schlegel, G. Farin, and C. Garbe, "Application of argon plasma coagulation in skin surgery." *Dermatology*, **197** (1998): 152-157.
13. Stalder, K.R., D.F. McMillen, and J. Woloszko, "Electrosurgical plasmas." *Journal of Physics D: Applied Physics*, **38** (2005): 1728-1738.

14. Stalder, K.R., J. Woloszko, I.G. Brown, and C.D. Smith, "Repetitive plasma discharges in saline solution." *Applied Physics Letters*, **79** (2001): 4503.
15. Carniol, P.J. and B.A. Greene, "What are the optimal techniques for skin rejuvenation?" *Archives of Otolaryngology -- Head and Neck Surgery*, **130** (2004): 1328-1333.
16. ArthroCare Corporation, *Coblation Explained*, http://www.arthrocare.com/our_technology/ot_coblation_explained.htm, as of March 2006.
17. Wright, N.T. and J.D. Humphrey, "Denaturation of collagen via heating: An irreversible rate process." *Annual Review of Biomedical Engineering*, **4** (2002): 109-128.
18. Windfuhr, J.P., J.C. Deck, and S. Remmert, "Hemorrhage following Coblation tonsillectomy." *Annals of Otology, Rhinology and Laryngology*, **114** (2005): 749-756.
19. Divi, V. and M. Benninger, "Postoperative tonsillectomy bleed: Coblation versus noncoblation." *Laryngoscope*, **115** (2005): 31-33.
20. Chang, K.W., "Randomized controlled trial of Coblation versus electrocautery tonsillectomy." *Otolaryngology - Head and Neck Surgery*, **132** (2005): 273-280.
21. Arya, A.K., A. Donne, and A. Nigam, "Double-blind randomized controlled study of Coblation tonsillotomy versus Coblation tonsillectomy on postoperative pain in children." *Clinical Otolaryngology*, **30** (2005): 226-229.
22. Rhytec, *The science of PSR^3: Thermal delivery*, http://www.portraitpsr.com/ph_science_delivery.html, as of
23. Sosnin, E.A., E. Stoffels, M.V. Erofeev, I.E. Kieft, and S.E. Kunts, "The effects of UV irradiation and gas plasma treatment on living mammalian cells and bacteria: a comparative approach." *IEEE Transactions on Plasma Science*, **32** (2004): 1544.
24. Kieft, I.E., J.L.V. Broers, V. Caubet-Hilloutou, D.W. Slaaf, F.C.S. Ramaekers, and E. Stoffels, "Electric discharge plasmas influence attachment of cultured CHO K1 cells." *Bioelectromagnetics*, **25** (2004): 362-368.
25. Sladek, R.E.J., E. Stoffels, R. Walraven, P.J.A. Tielbeek, and R.A. Koolhoven. "Investigation of possibilities of plasma treatment for dental caries." *2003*. 1109.
26. Sladek, R.E.J. and E. Stoffels, "Deactivation of *Escherichia coli* by the plasma needle." *Journal of Physics D: Applied Physics*, **38** (2005): 1716.
27. Goree, J., B. Liu, D. Drake, and E. Stoffels, "Disinfection of *S. mutans* bacteria using a plasma needle at atmospheric pressure." *To be published in IEEE Transactions on Plasma Science*, (2006).
28. Goree, J., B. Liu, and D. Drake, "Gas flow dependence for plasma-needle disinfection of *S. mutans* bacteria." *To be published in the Journal of Physics D: Applied Physics*, (2006).

29. Kieft, I.E., E.P.v.d. Laan, and E. Stoffels, "Electrical and optical characterization of the plasma needle." *New Journal of Physics*, **6** (2004): 149.
30. Laroussi, M. and X. Lu, "Room-temperature atmospheric pressure plasma plume for biomedical applications." *Applied Physics Letters*, **87** (2005): 113902.
31. Huyer, D.W. and S.H. Corkum, "Reducing the incidence of tap-water scalds: strategies for physicians." *Canadian Medical Association Journal*, **156** (1997): 841-844.
32. Léveillé, V., S. Coulombe, and S. Yonson. "Design and optimization of a miniature He-O_2 atmospheric pressure glow discharge torch for bio-applications." in *Proceedings of the 17th International Symposium on Plasma Chemistry, Toronto, 2005*. 346-347.
33. invitrogen, *Molecular probes - Generating and detecting reactive oxygen species*, http://probes.invitrogen.com/handbook/sections/1802.html, as of March 2006.
34. Halliwell, B. and J.M.C. Gutteridge, Free Radicals in Biology and Medicine. New York: Oxford University Press, 1999.
35. Moan, J., "On the diffusion length of singlet oxygen in cells and tissues." *Journal of Photochemistry and Photobiology, B: Biology*, **6** (1990): 343-347.
36. Pryor, W.A., "How lipid peroxidation works." *Free Radical Biology and Medicine*, **15** (1993): 536.
37. Mendez, I.J., W.J. Nicholson, and R.W. Taylor, "SOD isoforms and signalling in blood vessels: Evidence for the importance of ROS compartmentalization." *Arteriosclerosis, Thrombosis and Vascular Biology*, **25** (2005): 887-888.
38. Mikkelsen, R.B. and P. Wardman, "Biological chemistry of reactive oxygen and nitrogen and radiation-induced signal transduction mechanisms." *Oncogene*, **22** (2003): 5734-5754.
39. Alberts, B., D. Bray, J. Lewis, M. Raff, K. Roberts, and J.D. Watson, Molecular Biology of the Cell, 2nd ed., New York: Garland Publishing, 1989.
40. Introductory Biology Program, *Phospholipid*, http://www.biology.lsu.edu/introbio/Link2/phospholipid.gif, as of March 2006.
41. Lodish, H., A. Berk, P. Matsudaira, C.A. Kaiser, M. Kreiger, M.P. Scott, L. Zipursky, and J. Darnell, Molecular Cell Biology, 5th edition, W. H. Freeman, 2003. http://bcs.whfreeman.com/lodish5e/ as of March 2006
42. Watt, F.M., "Role of integrins in regulating epidermal adhesion, growth and differentiation." *EMBO Journal*, **21** (2002): 3919-3926.
43. Gough, J., *The cell*, http://personalpages.manchester.ac.uk/staff/j.gough/lectures/the_cell/cell_adhesion/page23.html, as of March 2006.
44. Roth, J.R., Industrial Plasma Engineering, Volume II: Applications to Nonthermal Plasma Processing. Vol. 2. London: Institute of Physics Publishing, 2001.

45. Laroussi, M., "Nonthermal decontamination of biological media by atmospheric-pressure plasmas: Review, analysis, and prospects." *IEEE Transactions on Plasma Science*, **30** (2002): 1409.
46. Larionov, P.M., A.N. Malov, M.M. Mandrik, N.A. Maslov, and A.M. Orishich, "Changes in the laser-induced fluorescence spectrum of myocardium tissue with decrease in its viability." *Journal of Applied Spectroscopy*, **70** (2003): 38.
47. Panjehpour, M., C. Julius, M.N. Phan, T. Vo-Dinh, and S. Overholt. "In vivo fluorescence spectroscopy for diagnosis of skin cancer." *2002*. 20.
48. Huang, Y., N.S. Sekhon, J. Borninski, N. Chen, and B. Rubinsky, "Instantaneous, quantitative single-cell viability assessment by electrical evaluation of cell membrane integrity with microfabricated devices." *Sensors and Actuators A: Physical*, **105** (2003): 31.
49. Lerouge, S., M.R. Wertheimer, and L.H. Yahia, "Plasma sterilization: A review of parameters, mechanisms, and limitations." *Plasmas and Polymers*, **6** (2001): 175.
50. Chau, T.T., K.C. Kao, G. Blank, and F. Madrid, "Microwave plasmas for low-temperature dry sterilization." *Biomaterials*, **17** (1996): 1273.
51. Kelly-Wintenberg, K., T.C. Montie, C. Brickman, J.R. Roth, A.K. Carr, K. Sorge, L. Wadsworth, and P. Tsai, "Room temperature sterilization of surfaces and fabrics with a one atmosphere uniform glow discharge plasma." *Journal of Industrial Microbiology & Biotechnology*, **20** (1998): 69.
52. Laroussi, M., F.C. Dobbs, and J. Paul Richardson, "Effects of nonequilibrium atmospheric pressure plasmas on the heterotrophic pathways of bacteria and on their cell morphology." *Applied Physics Letters*, **81** (2002): 772.
53. Weaver, J.C., "Electroporation of cells and tissues." *IEEE Transactions on Plasma Science*, **28** (2000): 24-33.
54. Zimmermann, U., U. Friedrich, H. Mussauer, P. Gessner, K. Hamel, and V. Sukhorukov, "Electromanipulation of mammalian cells: fundamentals and application." *IEEE Transactions on Plasma Science*, **28** (2000): 72-82.
55. Dev, S.B., D.P. Rabussay, G. Widera, and G. Hofmann, "Medical applications of electroporation." *IEEE Transactions on Plasma Science*, **28** (2000): 206-223.
56. Miyoshi, S., A. Ohkubo, N. Morikawa, Y. Ogawa, S. Nishimura, M. Fukugawa, H. Arakawa, J. Zenkou, and S. Sato. Method of transffering selected molecules. Patent US 2004/0110297 A1. June 10, 2004.
57. Sakai, Y., V. Khajoee, Y. Ogawa, K. Kusuhara, Y. Katayama, and T. Hara, "A novel transfection method for mammalian cells using gas plasma." *Journal of Biotechnology*, **121** (2006): 299-308.
58. Ogawa, Y., N. Morikawa, A. Ohkubo-Suzuki, S. Miyoshi, H. Arakawa, Y. Kita, and S. Nishimura, "An epoch-making application of discharge plasma phenomenon to gene-transfer." *Biotechnology and Bioengineering*, **92** (2005): 865-870.
59. Corning Incorporated, Corning cell culture selection guide. New York: Corning, 2005. 41.

60. BD Biosciences, BD Falcon (TM) cell culture products. Bedford: Beckton, Dickson and Company, 2001.
61. Brown, I.G., K.A. Bjornstad, E.A. Blakely, J.E. Galvin, O.R. Monteiro, and S. Sangyuenyongpipat, "Growth of large patterned arrays of neurons using plasma methods." *Plasma Physics and Controlled Fusion*, **45** (2003): 547-554.
62. Miller, C., H. Shanks, A. Witt, G. Rutkowski, and S. Mallapragada, "Oriented Schwann cell growth on micropatterned biodegradable polymer substrates." *Biomaterials*, **22** (2001): 1263-1269.
63. Schröder, K., A. Meyer-Plath, D. Keller, and A. Ohl, "On the applicability of plasma assisted chemical micropatterning to different polymeric biomaterials." *Plasmas and Polymers*, **7** (2002): 103-125.
64. Paikin, A., *VLSI*, http://www.hitequest.com/Kiss/VLSI.htm, as of March 2006.
65. Detrait, E., J.-B. Lhoest, B. Knoops, P. Bertrand, and P. van den Bosch de Aguilar, "Orientation of cell adhesion and growth on patterned heterogeneous polystyrene surface." *Journal of Neuroscience Methods*, **84** (1998): 193-204.
66. Lhoest, J.-B., E. Detrait, J.-L. Dewez, P. Van den Bosch de Aguilar, and P. Bertrand, "A new plasma-based method to promote cell adhesion on micrometric tracks on polystyrene substrates." *Journal of Biomaterials Science, Polymer Edition*, **7** (1996): 1039-1054.
67. Schröder, K., G. Babucke, and A. Ohl, "Visualization of a plasma-generated chemical micro-pattern on polystyrene by XPS." *Surface and Interface Analysis*, **36** (2004): 702-705.
68. De, S., R. Sharma, S. Trigwell, B. Laska, N. Ali, M.K. Mazumder, and J.L. Mehta, "Plasma treatment of polyurethane coating for improving endothelial cell growth and adhesion." *Journal of Biomaterials Science, Polymer Edition*, **16** (2005): 973-989.
69. Léveillé, V. "Design and characterization of an atmospheric pressure plasma torch for local biomedical applications." in *McGill Departmental Seminar Series, Montreal, 2004.*
70. Yamamoto, A., S. Mishima, N. Maruyama, and M. Sumita, "Quantitative evaluation of cell attachment to glass, polystyrene, and fibronectin- or collagen-coated polystyrene by measurement of cell adhesive shear force and cell detachment energy." *Journal of Biomedical Materials Research*, **50** (1999): 114-124.
71. Fox, M., D. Esveld, A. Valero, R. Luttge, H. Mastwijk, P. Bartels, A. van den Berg, and R. Boom, "Electroporation of cells in microfluidic devices: a review." *Analytical and Bioanalytical Chemistry*, (2006): 1.
72. Chen, W.E.I., "Electroconformational denaturation of membrane proteins." *Annals of the New York Academy of Sciences*, **1066** (2005): 92-105.
73. Radice, G.L. and M. Takeichi, *Cadherins*, in Cell Adhesion, M.C. Beckerle, Editor. 2001, Oxford University Press: New York. 62-99.

74. Panorchan, P., M.S. Thompson, K.J. Davis, Y. Tseng, K. Konstantopoulos, and D. Wirtz, "Single-molecule analysis of cadherin-mediated cell-cell adhesion." *Journal of Cell Science*, **119** (2006): 66-74.
75. Kokkoli, E., S.E. Ochsenhirt, and M. Tirrell, "Collective and single-molecule interactions of α5β1 integrins." *Langmuir*, **20** (2004): 2397-2404.
76. Yamamoto, A., S. Mishima, N. Maruyama, and M. Sumita, "A new technique for direct measurement of the shear force necessary to detach a cell from a material." *Biomaterials*, **19** (1998): 871-879.
77. Chu, Y.-S., W.A. Thomas, O. Eder, F. Pincet, E. Perez, J.P. Thiery, and S. Dufour, "Force measurements in E-cadherin-mediated cell doublets reveal rapid adhesion strengthened by actin cytoskeleton remodeling through Rac and Cdc42." *The Journal of Cell Biology*, **167** (2004): 1183-1194.
78. Curran, S.F., M.A. Amoruso, B.D. Goldstein, and R.A. Berg, "Degradation of soluble collagen by ozone or hydroxyl radicals." *FEBS Letters*, **176** (1984): 155-160.
79. Umebayashi, Y., Y. Miyamoto, M. Wakita, A. Kobayashi, and T. Nishisaka, "Elevation of plasma membrane permeability on laser irradiation of extracellular latex particles." *Journal of Biochemistry*, **134** (2003): 219-224.
80. Djordjevic, V.B., "Free radicals in cell biology." *International Review of Cytology*, **237** (2004): 57-89.
81. Clément, F., B. Held, N. Soulem, and C. Guimon, "XPS analyses of polystyrene thin films treated under DC pulsed discharges conditions in nitrogen, oxygen and oxygen-argon mixtures." *European Physical Journal: Applied Physics*, **18** (2002): 135-151.
82. Tamada, Y. and Y. Ikada, "Cell adhesion to plasma-treated polymer surfaces." *Polymer*, **34** (1993): 2208-2212.
83. Halliwell, B. and S. Chirico, "Lipid peroxidation: Its mechanism, measurement and significance." *The American Journal of Clinical Nutrition*, **57S** (1993): 715S-725S.
84. Templar, J., S.P. Kon, T.P. Milligan, D.J. Newman, and M.J. Raftery, "Increased plasma malondialdehyde levels in glomerular disease as determined by a fully validated HPLC method." *Nephrology Dialysis Transplantation*, **14** (1999): 946-951.
85. Takahashi, M., M. Shibata, and E. Niki, "Estimation of lipid peroxidation of live cells using a fluorescent probe, diphenyl-1-pyrenylphosphine." *Free Radical Biology and Medicine*, **31** (2001): 164-174.
86. Manevich, Y., T. Sweitzer, J.H. Pak, S.I. Feinstein, V. Muzykantov, and A.B. Fisher, "1-cys peroxiredoxin overexpression protects cells against phospholipid peroxidation-mediated membrane damage." *Proceedings of the National Academy of Sciences of the United States of America*, **99** (2002): 11599-11604.

Appendix 1. Cell treatment protocol

PREPARING THE TORCH

Before we start cell treatment, we want to figure out the operating conditions for the torch for the day. This needs to be done everyday as oxidation layers form, connections loosen, the capillary can shift, etc.

What we are looking for:

- Strong pinkish plasma jet (at least 1 mm long)
- Temperature < 40°C

Method:

1. Check to make sure everything is connected, and that all the connections are tight
    a. The capillary is secured in its fitting
    b. The copper wire is secured to the needle
    c. The ground and voltage probe are in contact with the epoxy
2. Turn on all electronics except the amplifier. Set properties on waveform generation (13.56 MHz, 100 Hz amplitude modulation, 0% depth), and start the modulator running. Leave electronics on for ½ hour before operating to avoid drift problems.
3. Open LabView™ "FrontPanel4" and press forward arrow at top left corner.
4. Open valves on gas cylinders. Make sure the output pressure is 30 psig (He) and 60 psig (O_2) and check to make sure there is still gas in the tank.
5. Set gas flow in LabView™ panel (1 slm He, 0.003 slm O_2), make sure measured value responds to set point. Check to make sure gas is flowing by temporarily blocking the nozzle exit with your finger – upon release you'll hear a whooshing noise.
6. Set PID value in LabView™, ~0.6 if you are using the tunable matching network.
7. Turn amplifier on to ¾ of the amplitude knob.
8. Check to see what your plasma jet looks like – you might have to turn off the lights.
9. Measure the temperature of the jet ~ 1 mm downstream from the nozzle exit. Make sure jet isn't arcing to thermocouple. If it is then increase distance. Move the thermocouple around in the jet until you find the maximum temperature.

Now: fiddle with the power to the jet (PID value) and the capillary position to get a strong jet at a low temperature. If the jet is purplish, it means the end of the capillary is most likely too far upstream from the nozzle exit. It is easier to move the quartz tube to adjust this factor, rather than the capillary itself.

If the temperature is less than 40°C, increase the power to maximize your potential of reactive species. If you find that you jump from say 33°C to 43°C, I would treat at 43°C, but try to keep the temperature below an absolute max of 45°C.

10. Once you have a pink jet at least 1 mm long and a temperature < 40°C, record the parameters (voltage, current, phase angle, PID, forward and reflected power, jet length and gas temperature).
11. Turn power off, stop gas flow by setting flow in LabView™ to 0.
12. Position the sample holder underneath the torch.
13. Place the Petri dish marked 'coated' on the holder.
14. Ensure that the scale on the vertical axis of the torch stage is positioned to a whole number, ie. 20 mm. Record this value.
15. Bring the sample holder up until the tip of the torch nozzle just touches the base of the Petri dish.
16. Use the vertical axis on the stage to raise the torch in order to remove the Petri dish from the holder.
17. The vertical axis of the torch is now zeroed in relation to the surface of the base of the Petri dish, allowing you to calculate the distance between the nozzle and the cells.

CELL PREPARATION AND PLASMA TREATMENT

Seed cells in 60 mm-diameter tissue culture Petri dishes - HepG2 cells at normal cell density, and HAAE-1 cells at high density if using late pass cells. Let the cells grow to confluence.

1. Warm media in incubator (volume will depend on experiments planned).
2. Once media is warm, remove confluent cells from incubator, rinse twice with PBS, and add ~ 2 mL of media to each 60 mm-diameter Petri dish.
3. Draw a line on the bottom of one Petri dish, through the centre of the dish. Mark one side with a G.
4. Put media back in incubator.
5. Wrap cells up in papertowel/tin foil, being sure to keep the cells level so the media doesn't spill.
6. Bring the cells, the 1 mL pipette and one 1 mL pipette tip down to the plasma torch.
7. Remove all of the media from the Petri dish using the pipette, and place it in the lid of the dish. Pipette the volume of media that corresponds with the optimized media height (h) back into the bottom of the dish.
   ie. 1.06 mL in 60 mm diameter dishes, h = 0.5 mm
8. Start gas flow using the LabView™ interface.
9. Place cells on sample holder underneath the plasma torch, and lower torch using the vertical stage so that the nozzle is 2 mm above the cells. (ie. if zeroed at 20 mm, lower torch to 18 mm).
   a. Be sure to constantly move the Petri dish while lowering the torch so that gas flow does not impinge on one area the whole time, detaching the cells. (the movement doesn't have to be super fast)

10. Once the torch is in place, move cells by hand on the side marked with a G, at about 3 s/cm. We are making sure that cells are not being detached due to the gas flow.
11. Once you've exposed the cells to the gas for a few tracks, move the Petri dish to cross over onto the other side of the line.
    a. Remember to keep the dish in constant motion!
12. Turn the plasma on (just turn the amp on, amplifier knob should not have been touched between set-up and experiment) to the PID value determined earlier, and expose cells on unmarked side of dish to plasma at a sweep speed of ~ 0.3 cm/s.
13. When the plasma treatment is finished, raise the torch using the vertical stage and remove Petri dish from holder. Keep moving the dish while you are raising the torch
    a. Again: extended exposure of one spot to the plasma/gas will cause cells to detach/desiccate.
14. Turn off amplifier and stop gas flow in LabView™.
15. Using the pipette, replace the media that is sitting in the lid back into the bottom of the Petri dish.
16. Wrap the cells up in papertowel/tin foil and bring them back to the laminar flow fume hood.
17. Look at Petri dish under the microscope, and make sure that there is minimal cell detachment on the side of the Petri dish that was only exposed to gas flow.
18. Transfer media with floating cells to a 35 mm-diameter Petri dish.
19. If you still want to use the cells left in the 60 mm-diameter dish, add more media. If not, throw it in the biohazard waste bin.
20. Check 35 mm dish under microscope to see if cells were successfully transplanted. About half the cells should have reattached. The other cells do not reattach after 24 hours.
21. Change the media in the 35 mm dish (~ 2 mL), and place in incubator.
22. Spray ethanol liberally everywhere where you brought the cells (5^{th} and 7^{th} floor), to try to keep everything relatively sterile.
23. Turn off electronics and close gas valves.

Appendix 2. Shear force calculation

The theoretical effect of the shear due to the gas flow on the cells is estimated (see details below). With a gas velocity of 100 m/s at the exit of the APGD-*t* nozzle, and a distance of 2 mm between the nozzle and the cells, the shear force applied on the cells is 29 nN (shear stress = 42 Pa). This calculation assumes that there is no media coverage on the cells.

Experimental data gives the strength of an individual $\alpha 5\beta 1$ integrin-ligand bond to be between 15 - 109 pN when using an AFM to pull the bond apart [1]. This is on the same order as the force required to remove an adhesion protein from the cell membrane and the cytoskeleton [2]. Researchers have also used a cantilever to measure the force required to push a cell to detach it from a surface. Yamamoto *et al.* used murine fibroblasts and found the shear strength required to detach the cells depended on the substrate on which the cells were grown, and varied from day to day [2, 3], but ranged from 420-1500 Pa (260-882 nN). An adhesion force of 297 nN on tissue culture PS most closely approximates the cell culture conditions used in these experiments. Sagvolden *et al.* [4] studied cervical carcinoma cells on treated polystyrene and found adhesion forces between 20-200 nN, depending on the surface treatment of the PS.

As the shear force exerted by the gas flow is less than the adhesion force of cells on tissue culture dishes, the theory dictates that the gas flow should not be able to remove cells on its own. However, if we include the effect of the media, the shear on the cells could be much higher. Water has a much higher viscosity than air, and the air impinging on the media is likely to create eddies and other flow patterns. The high shear force could result in cell detachment.

Calculation of the shear force on the cell due to the gas flow

Assumptions
- No media coverage on cells
- Newtonian fluid
- No slip at wall

Solved using theory on stagnation point flow to get maximum pressure at wall due to a uniform stream hitting a solid wall at a perpendicular angle.

$$\tau = \mu \frac{du}{dy} \qquad (1)$$

$$\tau = \mu \frac{\Delta u}{\Delta y} \qquad (2)$$

$$\tau = \mu \frac{\Delta(\frac{u}{U})}{\Delta(\sqrt{\frac{\alpha}{\nu}} y)} U \sqrt{\frac{\alpha}{\nu}} \qquad (3)$$

Where:

μ = viscosity of helium

$= 1.95 * 10^{-5} \frac{kg}{m \bullet s}$

u = velocity of the gas in the boundary layer above the impinging surface, f(x,y)

U = bulk gas flow parallel with impinging surface (taken as bulk gas velocity exiting the torch)

~ 100 m/s

α = positive rate of strain

ν = kinematic viscosity of helium

$= \frac{\mu}{\rho}$

ρ = density of helium

$= 0.1785 \frac{kg}{m^3}$

$\frac{\Delta(\frac{u}{U})}{\Delta(\sqrt{\frac{\alpha}{\nu}} y)}$ = slope of line tangent to $\frac{u}{U}$ at $\eta = 0$ (y = 0 at wall) in figure 5.6 [5] or 3.7 [6]

~ 1

Therefore:

$$\tau = 1.95 \times 10^{-5} \bullet 1 \bullet 100 \sqrt{\frac{\alpha}{\frac{1.95 \times 10^{-5}}{0.1785}}} \qquad (4)$$

But we're left with the ill-defined α term.

In [7] α is referred to as the positive rate of strain. This is the rate at which a material deforms, $\frac{du}{dx}$. Pohl *et al.* [8] describe it as a constant relating the velocity perpendicular to the wall with the distance from the wall. In the stagnation point flow diagrams, it is defined by the equations $U = \alpha x$ and $V = -\alpha y$ [5, 6].

Therefore, for V = 100 m/s (gas speed exiting the jet) at a distance y = 2 mm from the Petri dish,

$$\alpha = -\frac{100}{0.002}$$

As a is the positive rate of strain,

$$\alpha = \left|-\frac{100}{0.002}\right| = 50000 s^{-1}$$

Substituting back into (4)

$$\tau = 1.95\times10^{-5} \bullet 1 \bullet 100 \sqrt{\frac{50000}{\frac{1.95\times10^{-5}}{0.1785}}}$$

$$\tau = 41.7 \text{ Pa}$$

Therefore the force on the cell (assume average diameter = 30 μm)

$$\begin{aligned} F &= P \bullet A \\ &= 41.7 \bullet \pi r^2 \\ &= 41.7 \bullet \pi \bullet 0.000015^2 \\ &= 29 \text{ nN} \end{aligned}$$

1. Kokkoli, E., S.E. Ochsenhirt, and M. Tirrell, "Collective and single-molecule interactions of α5β1 integrins." *Langmuir*, **20** (2004): 2397-2404.
2. Yamamoto, A., *et al.*, "Quantitative evaluation of cell attachment to glass, polystyrene, and fibronectin- or collagen-coated polystyrene by measurement of cell adhesive shear force and cell detachment energy." *Journal of Biomedical Materials Research*, **50** (1999): 114-124.
3. Yamamoto, A., *et al.*, "A new technique for direct measurement of the shear force necessary to detach a cell from a material." *Biomaterials*, **19** (1998): 871-879.

4. Sagvolden, G., *et al.*, "Cell adhesion force microscopy." *Proceedings of the National Academy of Sciences of the United States of America*, **96** (1999): 471-476.
5. Schlichting, H., *et al.*, Boundary-Layer Theory, 8th ed., New York: Springer, 2000.
6. Kleinstreuer, C., Engineering Fluid Dynamics: An interdisciplinary systems approach. New York: Cambridge University Press, 1997.
7. Proudman, I. and K. Johnson, "Boundary-layer growth near a rear stagnation point." *The Journal of Fluid Mechanics*, **12** (1962): 161-168.
8. Pohl, P. and S.M. Saparov, "Solvent Drag across Gramicidin Channels Demonstrated by Microelectrodes." *Biophysical Journal*, **78** (2000): 2426-2434.

Appendix 3. Summary of attempted experiments

Table 1. Table of some experiments performed that require some adjustments to be successful, or are still in progress.

Experiment	What I was trying to prove	Why it didn't work
DPPP	• Stain for lipid peroxidation • Fluoresces when it binds with lipid peroxides	• Didn't have the proper fluorescent filters (excites 351nm, emits 380 nm) • Tried using DAPI filter (excitation 340-380 nm, suppression filter 425 nm), but blue fluorescence was non-specific, and intensity didn't increase after being exposed to light for 30 minutes • Got in contact with the people running the confocals/multiphotons on campus, and none of them had the appropriate filters. • One multiphoton could get to the high 300 nm range, but light source was photobleaching sample (part that was exposed to light beam showed increased fluorescence) • Can buy custom filters for a few hundred dollars (Chroma.com)
TBARS	• Quantify lipid peroxidation • TBA reacts with MDA, a secondary lipid peroxidation product, and the absorbance of the pink chromophore can be read at 532 nm	• 2-thiobarbituric acid (TBA) is a controlled substance • Need to get permits from Health Canada in order to use it, takes 3 months • Have chemicals/protocol required to test, just need the permit • Biggest problem will be the sample size. Need enough cells to get a detectable amount of MDA.

Attach a motor to the stage	• Ability to perform cell experiments with a known sweep speed • Motor turned stage at a constant speed through a series of gears and fittings, a power supply, a motor control board and a LabView™ interface • Motor control board needs to be cooled by a fan	• As stage allows precise axial movement, many rotations were needed to move the torch a few cm. • Took a few tries to find a motor with enough torque to turn the handle, max speed ~ 0.2 cm/s, slower than my operating sweep speed • At times, gears would catch; must securely align gears
Plasma treatment in a helium environment	• Isolate the effect of reactive helium species • Used quartz cross from CRDS reactor, and push/pull device to hold sample	• Vacuum leaks, likely due to teflon fittings holding needle in place From OES: • After purging overnight with helium at 20 Torr, increased nitrogen, OH, but almost no He, O detected (puzzling – alignment of OES checked and was at maximum) • After purging for 5 minutes, nitrogen levels decrease, helium and oxygen increase • If you add cells and evacuate for 5 minutes, still lots of evaporation from media, increase in O, OH
Online visualization of cell detachment	• Timescale for cell detachment • Brought inverted microscope from upstairs to the optical table, removed light source and replaced with light tube	• No video capture capabilities for the microscope that we have, took pictures once every 10 minutes • The pink media swirling around made it very hard to focus on the cells and get a clear picture.

Mouse Skin	• Effect of plasma torch on tissue • Penetration depth over specified treatment time • Obtained skin from wildtype mice	• Experiments done at the very beginning of thesis • Torch parameters not optimized, for the most part likely inflicting thermal damage on the skin • Shaving the mice sometimes resulted in damage to the epithelium, would want to use nude mice in the future
XPS	• Analyze the surface chemistry of the functionalized PS • Spin coated thin film of PS onto 13 x 17 mm Si wafers • Used 2wt% PS (Aldrich 18,242-7) in toluene • Increase in wt% increases film thickness • Spin coater parameters: t=20s, 3000 rpm, a=10 • Wafers dried overnight in a vacuum	• XPS kept breaking • Si coated wafers should be dried overnight in vacuum before functionalization • Functionalize < 3 days prior to analysis

McGill University

APPLICATION TO USE BIOHAZARDOUS MATERIALS*

Projects involving potentially biohazardous materials should not be commenced without approval from Environmental Health & Safety. Submit applications before 1) starting new projects, 2) renewing existing projects, or 3) changing the nature of the biohazardous materials within existing projects.

1. PRINCIPAL INVESTIGATOR: Richard L. Leask PHONE: ____

DEPARTMENT: Chemical Engineering FAX: ____

ADDRESS: ____ E-MAIL: ____

PROJECT TITLE: Miniature atmospheric pressure plasma torch for local biomedical applications

---

2. EMERGENCY: Person(s) designated to handle emergencies

Name: Richard Leask Phone No: work: ____ home: ____

Name: Alain Ganon Phone No: work: ____ home: ____

---

3. FUNDING SOURCE OR AGENCY (specify): NSERC I2I

Grant No.: TBA Beginning date: January 1 2006 End date: December 31 2007

. Indicate if this is

☐ Renewal: procedures previously approved without alterations.

Approval End Date: ____

☐ New funding source: project previously reviewed and approved under an application to another agency.

Agency: ____ Approval End Date: ____

☒ New project: project not previously reviewed.

☐ Approved project: change in biohazardous materials or procedures.

☐ Work/project involving biohazardous materials in teaching/diagnostics.

CERTIFICATION STATEMENT: Environmental Health & Safety approves the experimental procedures proposed and certifies with the applicant that the experiment will be in accordance with the principles outlined in Health Canada's "Laboratory Biosafety Guidelines" and in the "McGill Laboratory Biosafety Manual".

Containment Level (select one): ☐ 1 ☒ 2 ☐ 2 with additional precautions ☐ 3

Principal Investigator or course director: ____ (SIGNATURE) date: 12 (day) 01 (month) 06 (year)

Approved by Environmental Health & Safety: ____ (SIGNATURE) date: 17 (day) 01 (month) 06 (year)

Expiry: 31 (day) 12 (month) 07 (year)

*as defined in the "McGill Laboratory Biosafety Manual"

5: RESEARCH PERSONNEL: (attach additional sheets if preferred)

Name	Department	Job Title/Classification	Trained in the safe use of biological safety cabinets within the last 3 years? If yes, indicate training date
Sara Yonson	Chemical Engineering	MEng	Summer 2005
Andrea McGlynn	Chemical Engineering	MEng	Summer 2005

6. Briefly describe:

i) the biohazardous material involved (e.g. bacteria, viruses, human tissues, toxins of biological origin) & designated biosafety risk group

The affect of a non-thermal plasma torch on the attachment of mammalian cell cultures will be tested for potential biomedical applications (endothelial cells and HEP?G: biosafety level 1)

ii) the procedures involving biohazards

Cell culture (mammalian cells).

iii) the protocol for decontaminating spills

As per section 5.3 of the Mcgill biosafety manual.

1.Wear gloves and a laboratory coat or gown. Heavyweight, puncture-resistant utility gloves, such as those used for housecleaning and dishwashing..

2.Do not handle sharps with the hands. Clean up broken glass or other sharp objects with sheets of cardboard or other rigid, disposable material. If a broom and dustpan are used, they must be decontaminated later.

3.Avoid generating aerosols by sweeping.

4.Absorb the spill. Most disinfectants are less effective in the presence of high concentrations of protein, so absorb the bulk of the liquid before applying disinfectants. Use disposable absorbent material such as paper towels. After absorption of the liquid, dispose of all contaminated materials as waste.

5.Clean the spill site of all visible spilled material using an aqueous detergent solution (e.g., any household detergent). Absorb the bulk of the liquid to prevent dilution of the disinfectant.

Disinfect the spill site using an appropriate disinfectant, such as a household bleach solution. Flood the spill site or wipe it down with disposable towels soaked in the disinfectant.

7.Absorb the disinfectant or allow it to dry. 8.Rinse the spill site with water.

9.Dispose of all contaminated materials properly. Place them in a biohazard bag or other leakproof, labeled biohazard container for sterilization.

7. Does the protocol present conditions (e.g. handling of large volumes or high concentrations of pathogens) that could increase the hazards?

No

8. Do the specific procedures to be employed involving genetically engineered organisms have a history of safe use?
No

9. What precautions will be taken to reduce production of infectious droplets and aerosols?
All work will be conducted in a ~~laminar flow hood~~ and universal procotions will be observed.
biological safety cabinet

10. Will the biohazardous materials in this project expose members of the research team to any risks that might require special training, vaccination or other protective measures? If yes, please explain.

No

11. Will this project produce combined hazardous waste – i.e. radioactive biohazardous waste, biohazardous animal carcasses contaminated with toxic chemicals, etc.? If yes, please explain how disposal will be handled.
No

12. List the biological safety cabinets to be used.

Building	Room No.	Manufacturer	Model No.	Serial No.	Date Certified
Wong	7050	Thermo	1286	101513-2110	May 2005